

**Regulated flows influence on river morphodynamics:
The Spöl River (Swiss National Park)**

Master Thesis of the Faculty of Science of the University of Bern

submitted by

Salome Schläfli

2018

**Thesis Supervisor
Prof. F. Schlunegger**

**Thesis Co-Supervisor
Prof. M. Stoffel**

**Thesis Co-Supervisor
Dr. V. Ruiz-Villanueva**

Regulated flows influence on river morphodynamics: The Spöl River (Swiss National Park)

Master Thesis of the Faculty of Science of the University of Bern



Incorporated in
CH-6000

Long-term monitoring of fluvial morphology and related processes in the Spöl River
(Swiss National Park)

(http://4dweb.proclim.ch/4dcgi/parkforschung/de/Detail_Project?ch-6000)

Salome Schläfli*, Virginia Ruiz-Villanueva**, Samuel Wiesmann***, Ruedi Haller***,
Thomas Scheurer****, Fritz Schlunegger*, Markus Stoffel**

*Institut für Geologie, Universität Bern, Baltzerstrasse 1+3, CH-3012 Bern

**Institute for Environmental Science (ISE), University of Geneva, 66 Boulevard Carl-Vogt, CH-1205 Genève (markus.stoffel@unige.ch)

***Schweizerischer Nationalpark, Schloss Planta-Wildenberg, CH-7530 Zerneß

****ICAS – Internationale Kommission Alpenforschung, Haus der Akademien, Laupenstrasse 7, Postfach, 3001 Bern

u^b

**UNIVERSITÄT
BERN**



**UNIVERSITÉ
DE GENÈVE**

a^a swiss academies
of arts and sciences
ICAS - Interacademic Commission for Alpine Studies

**parc
nazional
svizzer**

Abstract

Natural morphodynamics of rivers has been altered for centuries through the regulation of their flow regimes. This paradigm in river management has changed over the course of the last few years, and in some cases, pioneering regime-based criteria have been applied to partially recover river integrity. One benchmark example is the Spöl River in the Swiss National Park (SNP), where a long-term artificial flood program started in 2000 (with the release of 2-3 high flows per year until 2017). One of the main purposes of this program was to improve geomorphic and therefore habitat heterogeneity in the river. After 16 years, many studies showed that the river recovered part of its mountain river character, and the artificial floods mitigated some of the effects of the river regulation. However, the morphodynamic effects are still not fully understood, and to date, there is no detailed geomorphic map of the Spöl River available. This research project aims to fill this gap and to improve the understanding of regulated flow effects on river morphodynamics. The main research questions of this study are related to the current heterogeneity of the fluvial forms and features and the use of unmanned aerial vehicles to gather high-resolution morphometric data. To answer these questions field and laboratory investigations are combined. Field surveys consist of field observations and measurements and unmanned aerial survey to gather hyperspatial imagery for the construction of high-accuracy digital surface models (DSM) and an orthophoto using photogrammetry with Agisoft Photoscan Pro. The approach contains the following steps: (1) a historical analysis of aerial pictures covering the period between 1946 and 2017, (2) a topographical sediment connectivity analysis at the watershed scale using the tool SedInConnect 2.3, (3) a grain size analysis along the upper Spöl River using photogranulometry and (4) a high-resolution characterization and mapping of the current geomorphology. The unmanned aerial surveys were carried out in summer 2017 using the AscTec Falcon 8 available at the SNP equipped with the RGB camera Sony Alpha NEX-7.

The geomorphic units are heterogeneously distributed along the upper Spöl River with some significant differences between wide and narrow subreaches, summarised in a conceptual model. Therein, narrow reaches are understood as transport efficient without major deposition, forming cascades of steps and pools. Wide reaches are dominated by depositional processes, forming bars and islands. The impact of the flood program is more obvious in wide reaches.

The historical analysis illustrates the impact of the dam construction and the flood program on the geomorphology of the Spöl River. The floods eroded the fans and flushed out the fine sediment fraction. Due to a lack of floods in 2017, fine sediment accumulated in the channel. Therefore, it is recommended to take up the frequent flooding of the upper Spöl River as soon as possible.

The sediment connectivity analysis highlights the fans and some tributaries as the main sediment sources for the upper Spöl River. Sediment input and erosion are assumed to have reached an equilibrium state. The stability of this equilibrium must be further investigated. If changes occur, the management strategies need to be adjusted to maintain the regained mountain river character of the Spöl River.

Content

1	Introduction	3
1.1	Research questions and Hypotheses	4
2	Study area	6
2.1	Site description	6
2.2	Flood program	9
3	Methods	10
3.1	Data acquisition	10
3.2	Historical analysis	11
3.3	Sediment connectivity analysis	15
3.4	Grain size analysis	17
3.5	High-resolution imagery survey	19
4	Results	23
4.1	Historical analysis	23
4.2	Sediment connectivity analysis	28
4.3	Grain size analysis	28
4.4	High-resolution imagery survey	30
5	Discussion	41
5.1	Methods	41
5.1.1	Historical analysis	41
5.1.2	Sediment connectivity analysis	41
5.1.3	Grain size analysis	42
5.1.4	High-resolution imagery survey	42
5.2	Results	44
5.2.1	Historical analysis	44
5.2.2	Sediment connectivity analysis	45
5.2.3	Grain size analysis	46
5.2.4	High-resolution imagery survey	46
5.3	Implications for flood management and river restoration	50
6	Conclusions	53
7	Acknowledgement	54
8	References	55
9	Appendix	62
9.1	Digital Appendix	62
9.2	List of Figures	63
9.3	List of Tables	65

1 Introduction

Natural morphodynamics of rivers has been altered for centuries through the regulation of their flow regimes. One of the main intervention in rivers is the construction of dams to store water for power production (World Commission on Dams, 2000; Nilsson et al., 2005) and to mitigate flood risk (Bravard and Petts, 1996; Wohl, 2006; Comiti, 2012). Dams affect the downstream flow regime in various ways. Commonly, they lead to a reduced fraction of fine sediment in upstream waters for it is deposited in the reservoir (Ward and Stanford, 1979). A common effect of flow regulation below dams is the alteration of habitat conditions, followed by ecosystem shifts (Graf, 2006). Abundant species get to dominate the system, resulting in a loss of biodiversity (Vinson, 2001).

In the past, the quest for security and stability to meet human needs largely overlooked the needs of aquatic ecosystems. But there is a change in river management towards regime-based management strategies with the aim to restore the affected river environment (Brierley and Fryirs, 2005). One frequently applied management strategy is the implementation of artificial floods. Fine sediment accumulates in gravels during low flow and, thus, clogs aquatic habitats. Artificial floods can be used to flush out fines and prevent the riverbed from clogging if sediment input from the reservoir is neglectable (Milhous, 1998; Mürle et al., 2003). Artificial floods in the Colorado River, Grand Canyon, were observed to revitalise fish habitats (Andrews and Pizzi, 2000; Schmidt et al., 2001). Mürle et al. (2003) documented that debris fans in the Spöl River were eroded already at discharges of 10 m³/s. However, the artificial flood procedure needs to be adapted to the individual stream system (Stanford et al., 1996, Milhous, 1998).

One benchmark example for adaptive river management in Switzerland is the Spöl River in the Swiss National Park (SNP). After the construction of the dam Punt dal Gall, the Spöl River remained as a residual stream what affected its morphodynamics downstream the dam (e.g. Mürle, 2000). A long-term artificial flood program was implemented in 2000 with the release of two to three high flows per year until 2017. One of the main purposes of this program was to improve habitat heterogeneity in the river. After 16 years, many studies showed that the river recovered part of its mountain river character, and the artificial floods mitigated some of the effects of the river regulation, mainly regarding ecology (Mürle et al., 2003; Uehlinger et al., 2003; Robinson and Uehlinger, 2006; Mannes et al., 2008). However, very few analysed the impacts of this regime on fluvial morphodynamics (Mürle et al., 2003; Pfäffli, 2013) and there is no detailed information about the spatial heterogeneity of the fluvial morphology so far.

A detailed fluvial geomorphic mapping is the basis to understand better river forms, patterns in their organisation, the processes producing and shaping those forms, or to interpret human-made interferences (Wheaton et al., 2015). Current and emerging technologies provide enormous opportunities to gather high-resolution data and to produce more accurate and detailed maps (Brasington et al., 2000; Bangen et

al., 2014; Wheaton et al., 2015). The present thesis is incorporated in a long-term monitoring of fluvial morphology and related processes in the Spöl River (Parkforschung, 01.04.2017). It aims to provide a detailed geomorphic map and improve the understanding of the current morphodynamics in the Spöl River.

1.1 Research questions and Hypotheses

The main research questions of this study are related to the current heterogeneity of the fluvial forms and features and the use of unmanned aerial vehicles to gather high-resolution morphometric data. The approach contains the following steps:

- a historical analysis of aerial images back to 1946 to reconstruct the changes in geomorphology due to the management of the river
- a sediment connectivity analysis on the watershed scale to identify the main sediment sources and estimate the linkage of the catchment to the channel
- a grain size analysis to assess the influence of the fans and tributaries regarding grain size distribution
- a high-resolution imagery survey with a drone and photogrammetry to analyse in detail the current morphology in the Spöl River

Regarding the geomorphic changes due to the dam construction and the flood program, we assumed the water channel area to decrease after dam construction and to increase with increasing flow dynamics with the flood program. Fans are anticipated to propagate into the river after dam construction for they are not eroded by high flows. After the start of the flood program, Mürle et al. (2003) observed erosion at the foot of fans. Therefore, we assumed that the total fan area decreases from 2000 to 2017.

Mürle et al. (2003) summarise the geomorphic characteristics of the Spöl River to be changed towards a more natural state by the artificial floods. Robinson and Uehlinger (2006) expect ongoing ecosystem regime shifts. We expected the Spöl River to show mountain river character after 16 years of the flood program. In wide and shallow reaches we expect sediment bars, wood and boulder deposition and riffles between bars (Brierley and Fryirs, 2005; Buffington and Montgomery, 2005). Sediment bars are expected to form downstream obstacles like wood and boulders (Keller et al., 1995), and linkage of wood and sediment storage is anticipated (Wohl and Scott, 2016). Narrow and steep reaches are expected to be confined, show bedrock outcrop and step-pool sequences (Buffington, 1997; Buffington and Montgomery, 1997).

Pfäffli (2013) documented the elevation changes from 2003 to 2009. He showed that the upper Spöl River underlies erosional processes since the flood program started. With a grain size analysis, he showed that the fans along the Spöl River are important sediment sources and influence the grain size distribution in the river. The downstream fining trend of the grain sizes is disturbed by steps in the pattern where fans occur. Compared to Mürle (2000) the mean grain size increased with the start of the flood program. We hypothesised to find a slightly increased mean grain size and

a similar pattern of grain size distribution along the Spöl River compared to Pfäffli (2013).

2 Study area

2.1 Site description

The study was carried out in the upper part of the Spöl River, which is located in the Swiss National Park (SNP) near Zernez in the eastern-most part of Switzerland (Figure 1). The SNP was founded in 1914 and is the oldest park in the European Alps. It covers an area of 170 km² from 1400 to 3173 m a.s.l. According to the International Union for Conservation of Nature IUCN, the SNP is a strict nature preserve of category 1a and thus a highly protected area. Together with the regional nature park Biosfera Val Muestair the SNP forms a UNESCO biosphere reserve (see the information brochure of the SNP in the Appendix, page 62).

The climate in the study area is continental with relatively low mean annual precipitation of 700 - 800 mm year⁻¹. It is characterised by high seasonal and daily variations in temperature with a mean annual value of 0.9 - 2.3°C (MeteoSwiss, 2018).

The Spöl River flows from the reservoir lake Lago di Livigno at 1745 m a.s.l. through Zernez into the Inn at 1470 m a.s.l., mainly orientated South-North. With a total length of 13.5 km, its mean slope is around 1 – 2%. It drains an area of 295 km² with a mean elevation of 2390 m a.s.l. (Mürle, 2000) (Table 1).

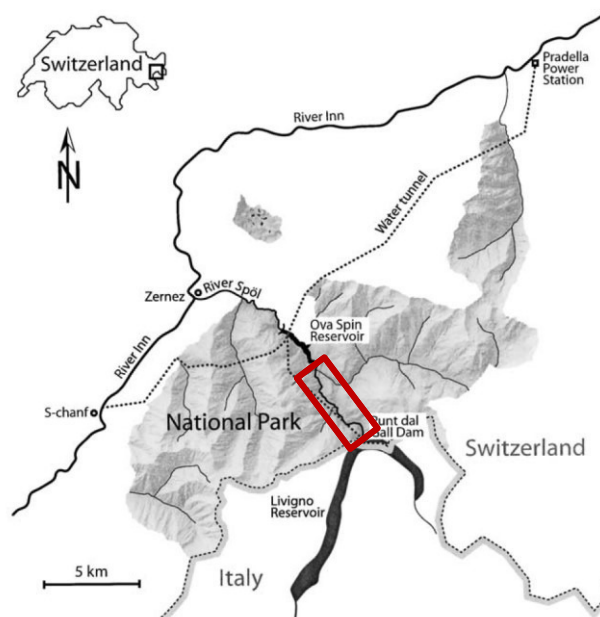


Figure 1: Overview of the study site (red rectangle) and surroundings (Scheurer and Molinari, 2003)

Table 1: river parameters

		Total	Punt dal Gall - Ova Spin
Length	[km]	14.7	5.5
Max. altitude	[m a.s.l.]	1745	1745
Min. altitude	[m a.s.l.]	1476	1640
Mean slope	[%]	1.83	1.84
Drainage area	[km ²]	434	185
Bare rocks	[%]	0.39	0.22
Coniferous forest	[%]	0.21	0.37

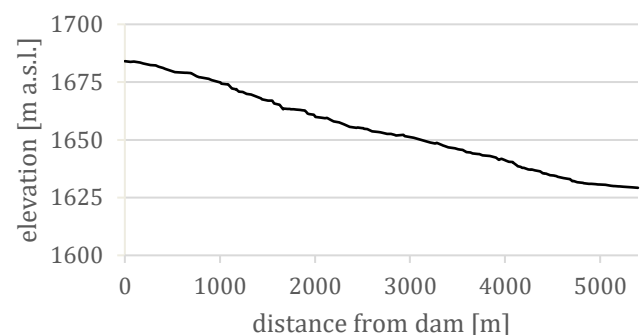


Figure 2: Longitudinal profile of the upper Spöl River from Punt dal Gall to Ova Spin

The study focuses on the upper part of the Spöl River between the reservoir lakes Lago di Livigno (1745 m a.s.l.) and Ova Spin (1640 m a.s.l.). From the dam of the upper reservoir lake, namely the dam Punt dal Gall, the Spöl River flows through a V-shaped valley, which was formerly glaciated and today shows canyon structures partly. Figure 2 shows a longitudinal profile of the studied reach from the dam Punt dal Gall to the reservoir lake Ova Spin. The solid rock walls confining the valley are mainly built of grey, banked dolomites and partly conglomerates of the Valatscha nappe in the sedimentary rocks of the eastern alpine (Figure 3). There is one bigger fault subparallel to the river and two crossing the valley. Two important tributaries reach the river close to one another and flow from south-west into the Spöl River near one of the valley-crossing faults, highlighted in Figure 3. The upstream tributary flows through the Val da l'Acqua and the downstream one through Val da la Foeglia. They are further referred to as "Acqua" and "Foeglia" river. A bit upstream the outlet of Acqua a change in geology occurs from dolomites to silt-, sand- and limestones. Narrow river sections are mainly confined by pure rock. There are many fans in the upper part of the river. The unconfined material on the slopes contains hillside debris, rockfall, and some moraine material. The main vegetation cover is coniferous forest. On the left side of the direction of flow, the vegetation cover of the catchment area gradually changes from coniferous forest over sparsely vegetated areas to bare rocks (Figure 4). The fluvial pattern of the river is characterised by pool-riffle sequences with some steps, at some points widening up with very calm flow, opposed to the narrow and deep canyons (Figure 5).

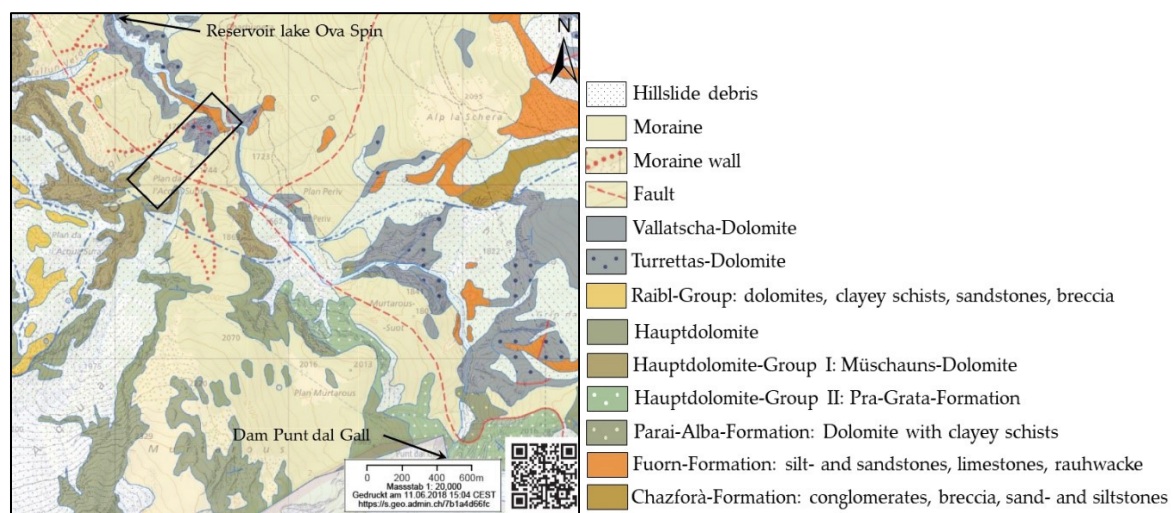


Figure 3: Geological map of the study area (swisstopo). The black rectangle highlights the outlets of Acqua and Foeglia (in flow direction) into the studied river reach

Study area

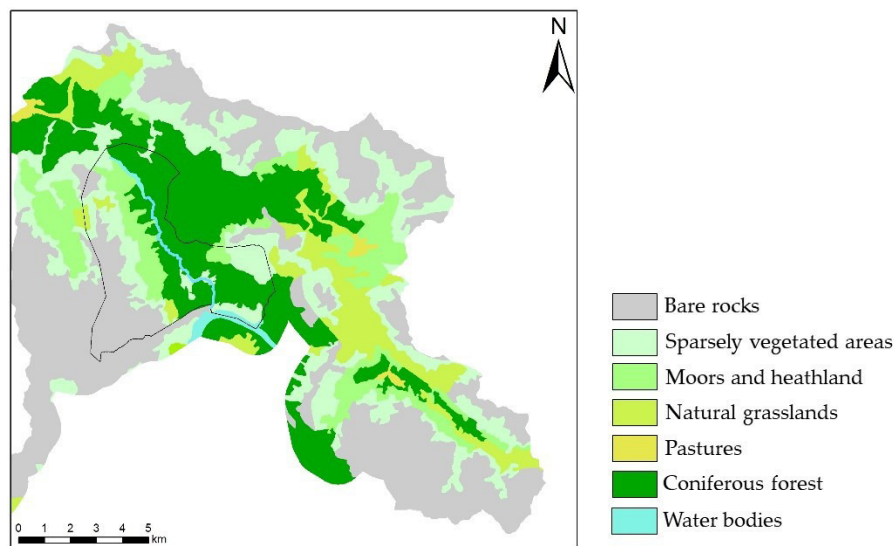


Figure 4: Corine Landuse Cover map for the catchment of the Spöl River on Swiss ground, a black line contours the reach from the dam Punt dal Gall to the reservoir lake Ova Spin



Figure 5: Impressions of the Spöl River, a-b) pool-riffle and steps, c-d) fans, e-f) canyons

2.2 Flood program

The hydropower generation is the only exception to the strict nature preserve requirements in the SNP. It was fixed in the foundation contract of the SNP (Schweizer Bund für Naturschutz, 1947). Before the construction of the dam Punt dal Gall the Spöl River was an alpine river with a nivo-pluvial flow regime with mean annual flows between 6.6 and $12.5 \text{ m}^3\text{s}^{-1}$ and floods reaching $20 - 60 \text{ m}^3\text{s}^{-1}$ (Mannes et al., 2008). In 1970, when dam construction was completed, the Spöl River remained as a residual stream with instream flow of $1 - 2 \text{ m}^3\text{s}^{-1}$. After this severe reduction following impacts on the river system were observed (Mürle, 2000):

- increase in fine material in the river bed
- changes in water temperature
- increasing algal production
- propagation of fans into the river bed

In the 1990s two major floods were released to empty the reservoirs. Some positive effects of these floods regarding ecology were observed in current monitoring projects (WNPK, 1991; Ackermann et al., 1996). These findings led to some experimental floods and finally to the start of the artificial flood program in 2000 (Scheurer and Molinari, 2003). In the framework of this program, two to three artificial floods are released per year (Figure 6). A reduction of the residual flow gathers the water for the floods. Therefore, the floods are cost-neutral (Mannes et al., 2008).

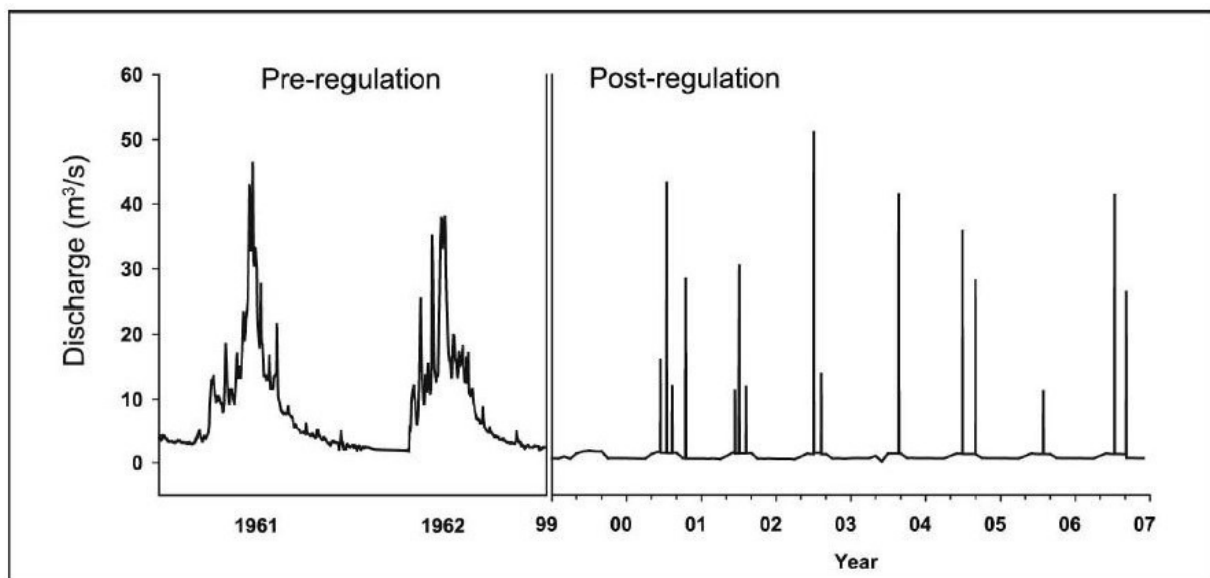


Figure 6: Flow regime of the Spöl River before dam construction (1961 and 1962), after dam construction (1999) and during the flood program (2000-2006). The flow in 1999 represents the residual flow maintained below the dam with all excess water diverted downstream for power production (Mannes et al., 2008)

3 Methods

In the approach of this thesis field and laboratory investigations are combined. To get insight into the temporal evolution of the studied river reach a historical analysis of aerial images back to 1946 was implemented. A connectivity analysis on the watershed scale helps to improve the understanding of the sediment processes. A grain size analysis was carried out to analyse the influence of different sediment sources. Hyperspatial imagery was taken with the help of a drone to generate a DSM and an orthomosaic. This allows a high-resolution characterisation of the current morphology validated with field measurements. As a final result, a detailed geomorphic map of the Spöl River is created from which a conceptual model can be extracted. Figure 7 gives an overview of the applied approach.

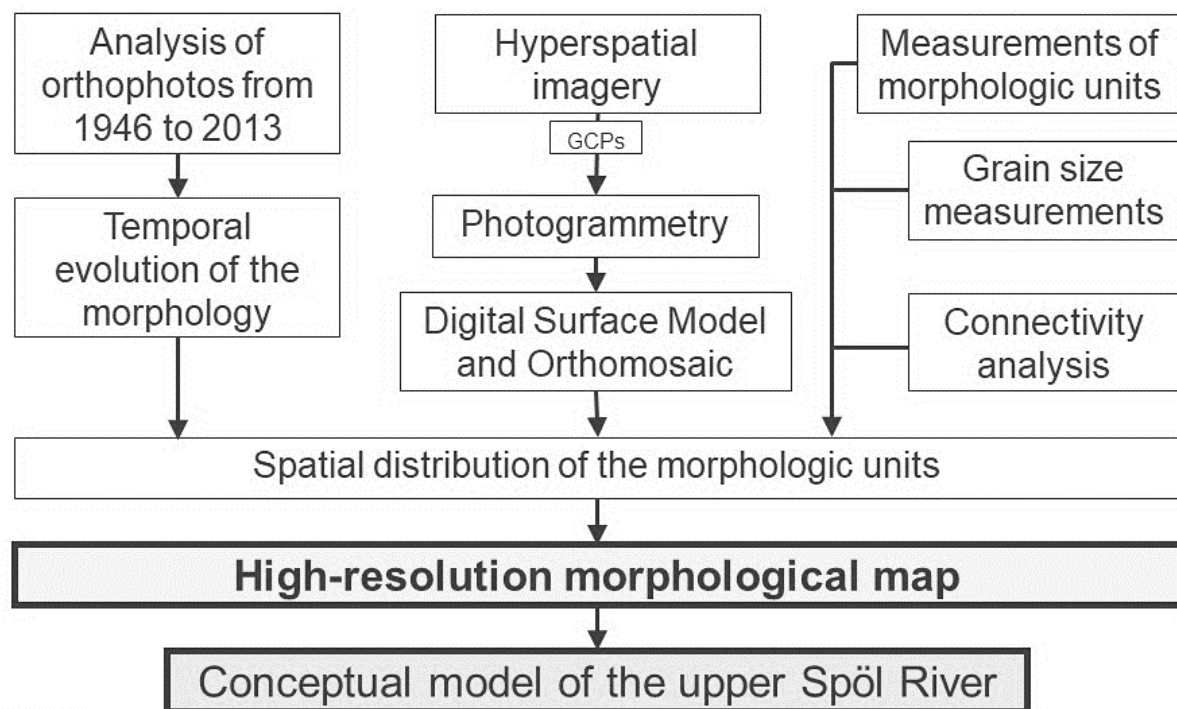


Figure 7: General flow chart with the applied approach

3.1 Data acquisition

The historical analysis is based on orthomosaics listed in Table 2. All of them were provided by the SNP. The Digital Elevation Model (DEM) for the connectivity analysis is extracted from the swissALTI3D, a digital elevation model from the Federal Office of Topography with a grid size of 2 x 2. The most recent update of this DEM in the study area is from 2009. More details are found in the Appendix (page 62).

Table 2: Overview of the analysed orthomosaics with project parameters

Year	Shooting date	Grid size [X, Y]	project
1946	summer 1946	100, 100	worldwide mapping project of the USAF
1988	07.08.1988	40, 40	Geodetic survey for the SNP
2000	24.08.2000	20, 20	aerial survey for the SNP
2009	20.06.2009	10, 10	aerial survey regarding the emptying of the reservoir lake Ova Spin in the SNP
2010	13.10.2010	25, 25	SWISSIMAGE 2010 orthomosaic from the Federal Office of Topography
2013	23.09. / 04.10.2013	25, 25	SWISSIMAGE 2013 orthomosaic from the Federal Office of Topography
2017	18.07. / 21. - 23.08.2017	1.7, 1.2	aerial survey within a long-term monitoring project along the Spöl River (CH-6000)

3.2 Historical analysis

A geomorphic unit is defined as a landform induced by deposition and/or erosion of sediment and bedrock (Wheaton et al., 2015). The geomorphic units of the river were manually classified and mapped on seven orthomosaics of different ages (listed in Table 2) using ArcGIS. Figure 8 illustrates the detailed classification framework. The classification is adapted from Demarchi et al. (2016). First, the reach is divided into Flood-Plain units (FP) and the Total Active Channel (TAC). FP include everything that is not reworked by floods. The TAC is further divided into Sparsely-Vegetated units (SV) and units without vegetation, namely the Active Channel (AC). The AC is divided into the low-flow Water Channel (WC) and Unvegetated Sediment units (US). The division into FP, SV, US, and WC helps to understand the morphodynamics in the river regarding the reworking through floods. WC and US are continuously reworked by smaller floods, SV only by higher floods, indicated by the development of vegetation. The geomorphology on FP is not primarily influenced by floods, and hence vegetation can condense. FP can be subdivided into Densely-Vegetated units of Islands (DVI), Riparian Densely-Vegetated units (RDV), fans and debris cones (fan) and Other Floodplain Units (OFU). SV contain sparsely-vegetated riparian units (RSV) and islands (SVI). US are subdivided into mid-channel (mcb), lateral (lb) and point bars (pb). The WC is subdivided into pools (P), riffles (Ri), runs (Ru), standing water (StW) and waterfalls

Methods

(Wf) (Figure 9). As In-Channel-Features (ICF) boulder (bo), wood logs (log) and wood jams (jam) were identified. All subclasses are described in detail in Table 2.

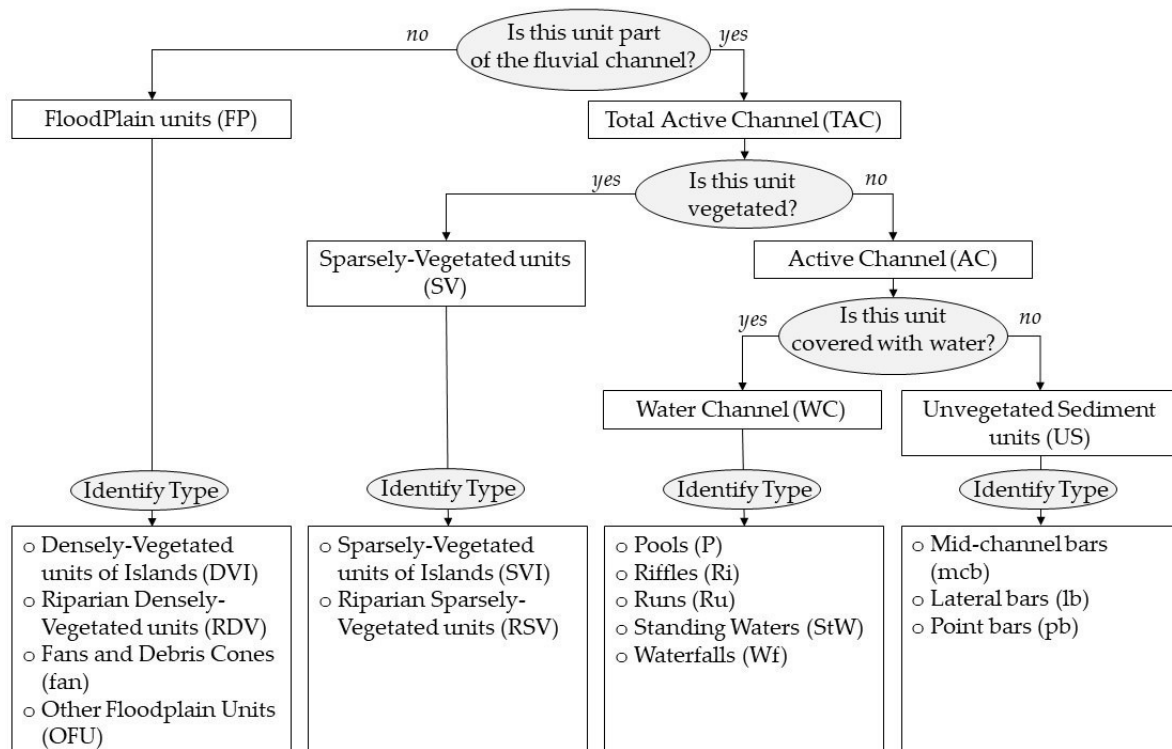


Figure 8: Classification framework



Figure 9: Example of the mapped units in the Spöl River (without ICF)

Table 3: Classification scheme, adapted from Demarchi et al. (2016)

Class		Class description
Water Channel (WC) - part of the Active Channel (AC)	Pools (P)	Areas with a gentle surface slope and slow flow
	Riffles (Ri)	Areas of swifter-flowing water
	Runs (Ru)	Areas of fast-moving, non-turbulent flow
	Standing Waters (StW)	Surface water relatively still
	Waterfall (Wf)	Step or waterfall
	Unclassified Water surface (uncW)	Areas of undetectable water surface (e.g., shadows, image blur)
Unvegetated Sediment bars (US) - part of the Active Channel (AC)	mid-channel bar (mcb)	Sediment bars without vegetation entirely surrounded by WC
	lateral bar (lb)	Straight sediment bars without vegetation adjacent to (but not surrounded by) WC
	point bar (pb)	Curved sediment bars without vegetation adjacent to (but not surrounded by) WC
Sparsely-Vegetated units (SV) – part of the Total Active Channel (TAC)	Sparsely-Vegetated units of Islands (SVI)	Sparse vegetation units entirely surrounded by WC and/or US
	Riparian Sparsely-Vegetated units (RSV)	Riparian sparse vegetation units adjacent to (but not surrounded by) WC and/or US
FloodPlain units (FP)	Densely-Vegetated units of Island (DVI)	Dense vegetation units entirely surrounded by WC and/or US and/or SVI
	Riparian Densely-Vegetated units (RDV)	Riparian dense vegetation units adjacent to (but not surrounded by) WC and/or US and/or RSV
	Fans and Debris Cones (fan)	Cone-shaped sediment accumulation
	Other Floodplain Units (OFU)	All remaining floodplain units
In-Channel Features (ICF)	Boulders (bo)	big rocks inside WC and/or US
	Wood Logs (log)	A single wood piece inside WC and/or US
	Wood Jams (jam)	wood accumulation inside WC and/or US

To validate the manual classification on the orthomosaics field measurements were taken. The field measurements include GPS measurements of the position of geomorphic units and dimension measurements like the length and width of bars, the channel width and the dimensions of some big boulders (Figure 10). The field measurements and the mapped units have been compared qualitatively to assure a con-

Methods

sistent classification. A Spearman test (Kendall, 1970) was used to validate the correlation between field and remote mapping. The subdivision of the studied reach into 25 subreaches of 40 – 540 m length was defined by field observation of striking changes in flow type and geomorphology and determined by GPS measurements (Table 4).



Figure 10: Field measurements for validating the remotely mapped units (a) boulder dimensions and wood jam, b) pool depth, c) wood log, d) subreach boundary)

Table 4: Subreach description

Subreach Nr.	Distance from dam [m]	Length [m]	Description
1	0	58	Outlet, pool
2	58	214	riffles, shallow
3	272	153	riffles with some pools
4	426	207	Discharge measurement installation, gorge, pool with some riffles
5	633	452	riffles with some pools, shallow
6	1085	196	pool-step, bedrock in the riverbed
7	1282	270	pool-riffle, bedrock in the riverbed
8	1552	114	pool-step, bedrock in the riverbed
9	1666	46	gorge, deep, quiet
10	1712	273	riffles, wide, shallow
11	1985	380	pool-riffle
12	2364	85	gorge, deep, quiet
13	2450	350	riffles with some pools
14	2800	538	pool-riffle and bars, curves, change in geology (conglomerate boulders)
15	3338	258	riffles and bars
16	3596	339	pool-riffle and bars, curves
17	3936	197	riffles and bars, wide, braided-like
18	4133	141	pool-riffle, narrow, deep
19	4274	267	pool-riffle, shallow, vegetated bars
20	4541	141	riffles, wide, shallow
21	4681	39	pool-step, bedrock in the riverbed
22	4721	180	riffles with some pools
23	4901	342	riffles and bars
24	5243	155	weak flow, influenced by stowage of reservoir lake Ova Spin, widening, deepening
25	5397	99	standing water, stowage of reservoir lake Ova Spin

3.3 Sediment connectivity analysis

A sediment connectivity analysis was carried out to identify the sediment sources along the Spöl River. Cavalli et al. (2013) define sediment connectivity as the degree of linkage that controls sediment fluxes throughout landscapes and in particular between sediment sources and downstream areas. In this study, an index of connectivity (IC) was modelled with the stand-alone application developed by Cavalli et al. (2014) (SedInConnect 2.4). Based on the approach of Borselli et al. (2008) with some modifications to adapt the model to mountain catchments, this method permits a rapid and simple investigation of the potential linkage for sediment processes in an alpine environment (Messenzehl et al., 2014).

The IC is defined as:

$$IC = \log_{10} \left(\frac{D_{up}}{D_{dn}} \right) = \log_{10} \left(\frac{\bar{W} \bar{S} \sqrt{A}}{\sum_i \frac{d_i}{W_i S_i}} \right) \quad (1)$$

with a downslope (D_{dn}) and an upslope (D_{up}) component of connectivity (Figure 11). D_{up} is defined by a dimensionless weighting factor \bar{W} , the average slope gradients \bar{S} [m m^{-1}] and the upslope contributing area A [m^2]. D_{dn} contains the length d_i [m] of the flow path along the i^{th} cell according to the steepest downslope direction. W_i and S_i are the weighting factor and the slope gradient of the i^{th} cell, respectively. The connectivity increases with an increasing IC (Borselli et al., 2008).

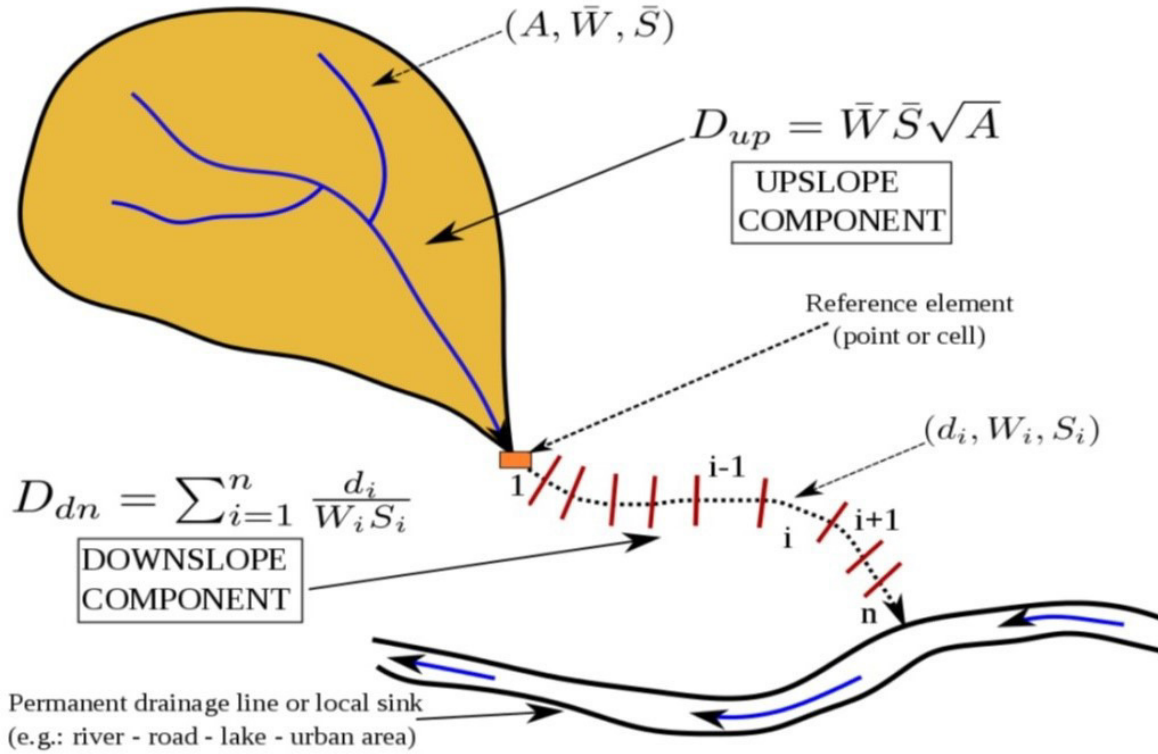


Figure 11: Upslope and downslope components of the IC (Cavalli et al., 2014)

As input parameters for the connectivity analysis in the upper Spöl River, the DEM from swissALTI3D was used after being processed with the Pit Remove algorithm of TauDEM (Tarboton, 2012). We used a polygon mask of the river channel as a target. Cavalli et al. (2013) propose to use the following expression as a weighting factor \bar{W} :

$$W = 1 - \left(\frac{RI}{RI_{MAX}} \right) \quad (2)$$

with RI as the roughness index defined as:

$$RI = \sqrt{\frac{\sum_{i=1}^{25} (x_i - x_m)^2}{25}} \quad (3)$$

The RI is a good weighting factor for alpine catchments for it considers differences of bare areas like outcropping rock and debris cover. In contrast, the originally proposed C-factor is based on vegetation cover which may be very useful for agricultural and forest environments but is not compulsory informative regarding the connectivity in alpine catchments (Cavalli et al., 2014).

Further the RI as a weighting factor \bar{W} was normalized as proposed in Trevisani et al. (2016). For smoothing the original DEM, a moving window of 5 pixels was introduced and the input cell size was set to be 2 map units pursuant to the DEM.

To compare the IC with geomorphic features like fans the orthomosaic from 2009 was consulted for it has the same age as the used swissALTI3D. A Kruskal-Wallis test (Kruskal and Wallis, 1952) was used to verify whether the distribution of mapped units or measurements differs significantly between groups of location.

3.4 Grain size analysis

Grain Size Distribution (GSD) measurements along a river can be a proxy for the sediment impact of different sediment sources. In general, the fine fraction gets transported further downstream. Therefore, the GSD shows a fining trend downstream a river (Kondolf et al., 2005). Changes against this trend or big changes over a short distance (steps in the downstream pattern) are indicators for factors which affect the grain size pattern like tributaries and other sediment inputs (Rice and Church, 1998).

Photographic grid sampling is a simple and rapid method to gather samples of GSD. Pictures were taken perpendicularly to 17 gravel bars along the studied reach with a double meter forming a frame for scale. With ImageJ, an open source image processing program, a grid was projected on the images (Figure 12). For each grain underlying a grid cross, the intermediate b-axis was measured. It was assumed that the grains lay perpendicular to their shortest axis (c-axis) and the b-axis corresponds to the shorter visible axis (Kellerhals and Bray, 1971).

Methods



Figure 12: Example of a GSD picture with the overlying grid in ImageJ

In addition, a grain size analysis from Pfäffli (2013) was consulted. To ensure comparability between the two analyses the transformation and evaluation of the measurements was taken over from Pfäffli (2013). The approach largely follows Bezolla (2013).

The measurements are grouped into grain size classes proposed by Pfäffli (2013). Grains smaller than 1 cm are neglected. This fraction will be added later using a Fuller-distribution (Fehr, 1987). The grain size classes have to be transformed from distribution samples to volume samples as follows:

$$\Delta p_i = \frac{\Delta q_i d_{mi}^{0.8}}{\sum_1^N q_i d_{mi}^{0.8}} \quad (4)$$

with Δp_i as the relative weight of fraction i, Δq_i as the relative number of fraction i, d_{mi} as the mean grain diameter of fraction i and N as the total number of fractions.

Now a correction for the grains smaller than 1 cm is implemented, assuming 25% of the grains in the study area belong to this class:

$$p_{ic} = 0.25 + 0.75 \sum_1^i \Delta p_i \quad (5)$$

with Δp_{ic} being the corrected cumulative frequency of fraction i.

The distribution of the fine grains (smaller than 1 cm) is approximated with a Fuller distribution. The transition between the two distributions has to be set to a point where they have the same tangential slope. The procedure to find a good transition point is somehow subjective with the following calculations as background:

$$p_{FU(i+1)} = \sqrt{\frac{d_{i+1}}{d_{maxFU}}} \quad \text{with } d_{maxFU} = \frac{d_i}{p_{ic}^2} \quad (6)$$

$$p_{FU(i)} = \sqrt{\frac{d_i}{d_{maxFU}}} \quad \text{with } d_{maxFU} = \frac{d_u}{p_{uc}^2}$$

with $p_{FU(i)}$ as the Fuller distribution of fraction i , approximated in a first step with the grain diameter of the previous fraction. Subsequently, u is defined as the fraction where $p_{FU(i)}$ and p_{ic} are the closest and the final Fuller distribution is calculated with u defining d_{maxFU} .

With a Pebble Count Analyzer provided by Commonwealth of Kentucky (Ky.gov, 28.02.2018), variable characteristic grain size diameters can be calculated for further analyses. For further comparison between the GSD along the river in 2013 and 2017, respectively, the mean grain diameter (d_m) and the d_{90} were calculated. A Mann-Whitney test (Hollander and Wolfe, 1999) was used to verify whether d_m and d_{90} differ significantly between 2013 and 2017.

3.5 High-resolution imagery survey

The unmanned aerial data gathering was done using the AscTec Falcon 8 available at the SNP. The octocopter is equipped with the RGB camera Sony Alpha NEX-7. The planning of the flights was done with AscTec Navigator V3.4.4, the navigation software corresponding to the drone (Figure 13). The flight height was set to 50 m with a velocity of 3.5 m s^{-1} . From experience, the calculated velocity from the AscTecNavigator of 5.77 m s^{-1} is too fast. The minimal overlap of the images was forced to be 80% to enable photogrammetry in the post-process. The path was planned as a line with matrix waypoints to be followed during the flights. It is important to check that there are no red blinking sections and no loops in the planned path. If so, the waypoints need to be adjusted until every line section is straight and at least yellow. To cover the whole reach 24 flights of 200 – 500 m length (20 – 50 waypoints) were carried out. The waypoints are manually deactivated before starting the flight. Otherwise, the drone would stop at every point, unnecessarily extending the flight time for approximately 10 s per waypoint. The length of the flights was limited by the condition of continuous visibility of the drone during the remote control. The flight plans overlapped each other at the ends to ensure continuous coverage of the reach.

Methods

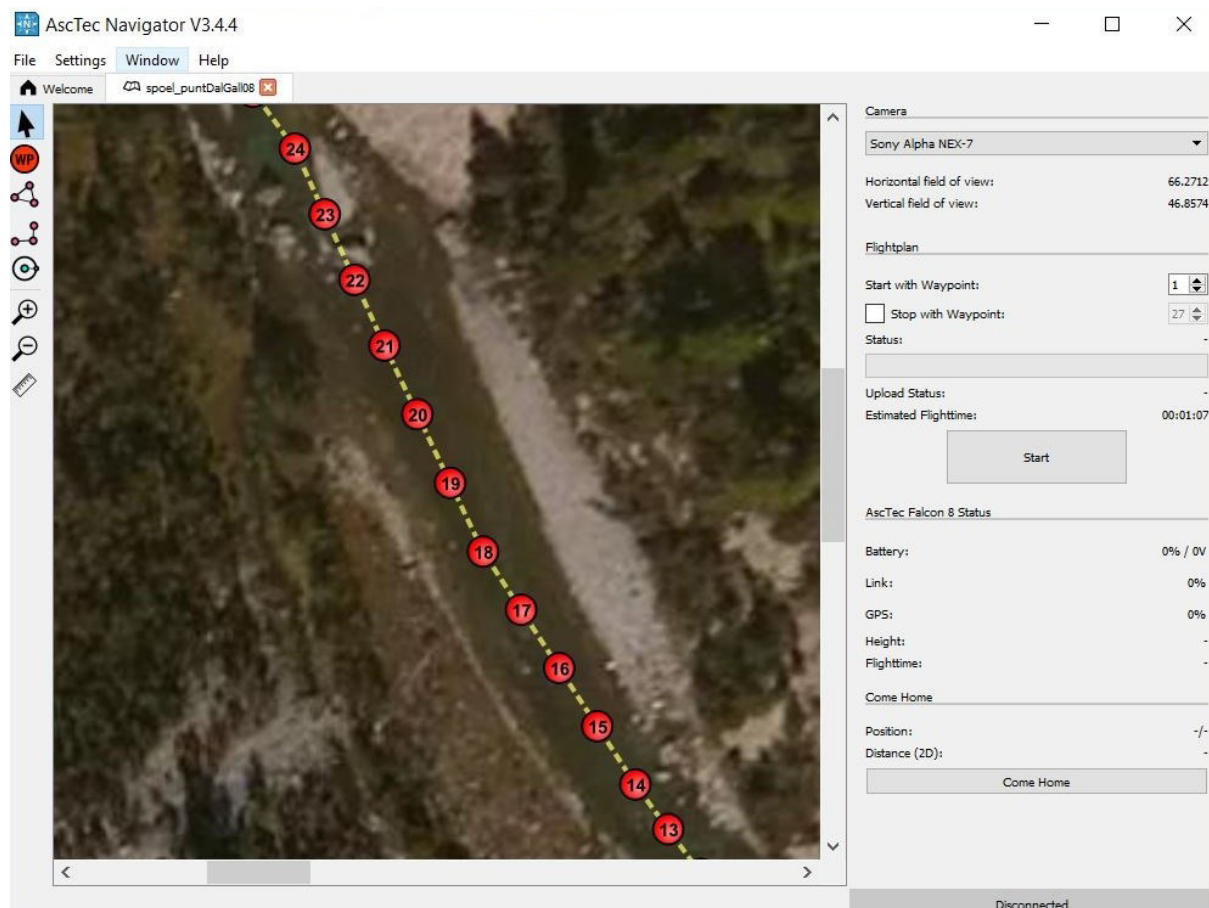


Figure 13: Flight plan in AscTec Navigator

In the field, a proper site to launch and land the drone has to be found. The AscTec Falcon 8 can be started out of the hand of someone holding it up high. For landing one can operate it down vertically by remote control and catch it from the air manually. The flight height had to be adapted in the field for some flights as the starting site was located on a higher elevation than the river.

In total six field days were needed to cover the whole reach including installation and measurement of Ground Control Points (GCP) and field observations for completion. Bright plastic targets of 10 x 10 cm were used as GCP's. They were installed in a zigzag line every 50 m at good visible sites on both sides of the river by fixing them to the underground with nails or metal clamps. The GPS measurements were done using a Trimble Geo XR in combination with an external antenna ("Zephyr-Model 2"). The measuring of the GCP's was done some weeks after the flight due to a technical defect. In the meantime, some GCP's were flushed away. As a replacement prominent points in the landscape were measured. When the GCP was installed above ground, the height was noted. Figure 14 gives some impressions of the fieldwork with the drone.



Figure 14: Fieldwork with the drone: a)-b) AscTec Falcon 8 octocopter, c) starting the drone by hand, d) remote control of the previously planned flight, e)-f) GCP installation and measuring

The RGB imagery was imported into Agisoft Photoscan Professional Edition 1.3.4 to generate a high-resolution orthomosaic and a DSM by means of the Structure-from-Motion photogrammetric approach (SfM). SfM is an automated image-based surface restitution method. By matching a series of overlapping images, a 3D geometry can be generated (Figure 15) (Woodget et al., 2017).

The processing of the orthomosaic and the DSM largely follows the tutorial “Orthophoto and DEM Generation (with GCPs)” provided by agisoft.com (06.11.2017). To reduce processing time the flights are processed one at a time and aligned afterwards.

Methods

In a first step, the images are aligned, and a mesh is generated from a sparse cloud. Then the GCPs are identified and marked. After importing the coordinates of the GCPs, a dense cloud is generated, and the mesh is updated. Close to the reservoir lake Ova Spin, the reach was impassable, and therefore GCPs are missing. They are remotely added during the processing to match the images, but exact coordinates are missing. After some editing (closing holes, decimating mesh) a texture is built. Now the dense clouds of the single flights can be merged to one dense cloud from which the DSM and the orthomosaic can be generated and finally exported to ArcGIS for further analyses.

The orthomosaic together with the DSM allow the identification, classification, and mapping of the main fluvial features. This approach has been rapidly spread in the field of fluvial geomorphology (Bangen et al., 2014). To generate a high-resolution geomorphic map of the upper Spöl River, the same classification units as for the historical analysis are used (Table 2). Additionally, channel and valley width were measured approximately every 50 m. The channel width was defined to include the TAC. The valley width was estimated on profiles through the swissALTI3D along the channel width measurements by identifying changes in the slope that indicate the transition from valley to channel. The fan width was measured at the contact of the fan with the river. To evaluate if a correlation between mapped units is significant a Spearman test was used (Kendall, 1970). A Kruskal-Wallis test (Kruskal and Wallis, 1952) was used to verify whether the distribution of mapped units or measurements differs significantly between groups of location.

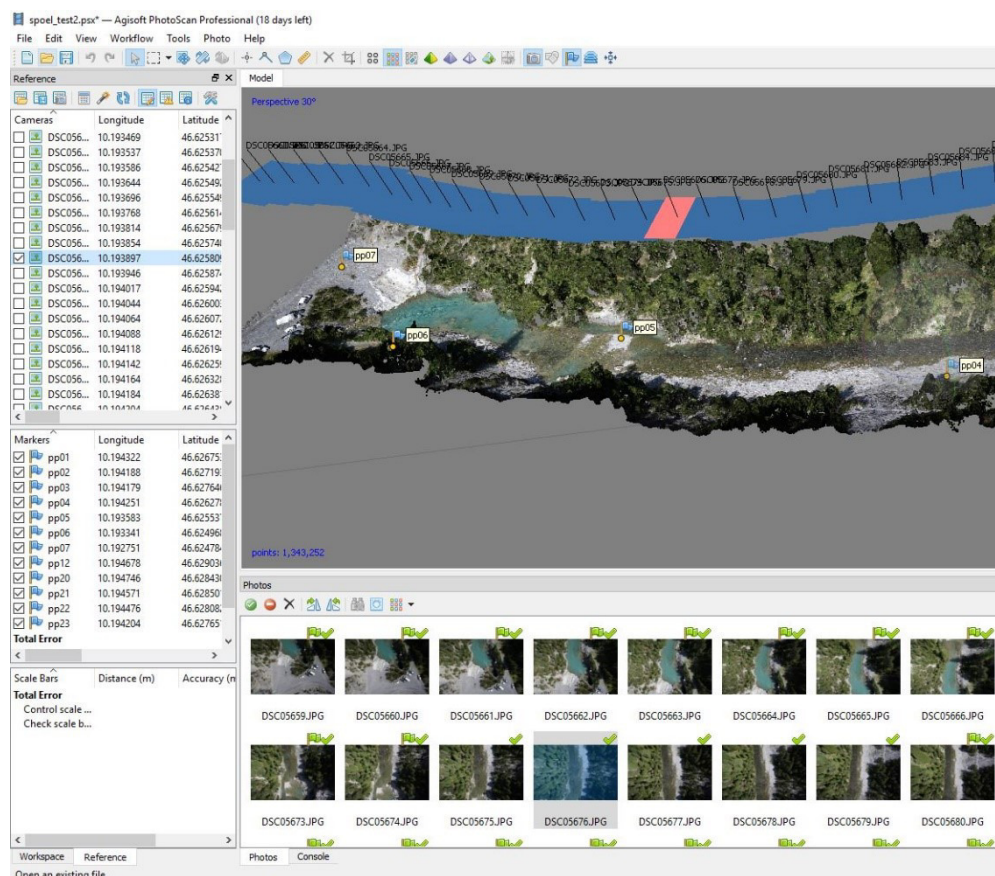


Figure 15: Post-processing of the aerial imagery in Agisoft Photoscan

4 Results

4.1 Historical analysis

The geomorphic mapping on the orthomosaics of different ages reveals a temporal evolution of the geomorphic units in the Spöl River from before dam construction to 17 years after the start of the flood program. Figure 16 gives an overview of the development of the main geomorphic units over time. It shows water channel, sediment bars and fan area with the annual maximum discharge. Fan and sediment bar area increase from dam construction (1970) to the start of the flood program (2000) while water channel area decreases in this time span. After the year 2000 fan area shows a decreasing trend. Sediment bar and channel area show an indistinct course after the start of the flood program but are somehow mirror-inverted to each other with an outstanding peak in the year 2009 (high peak for water channel, low peak for sediment bar area). Additionally, we observed some large wood logs and boulders lying at the same location on all orthomosaics.

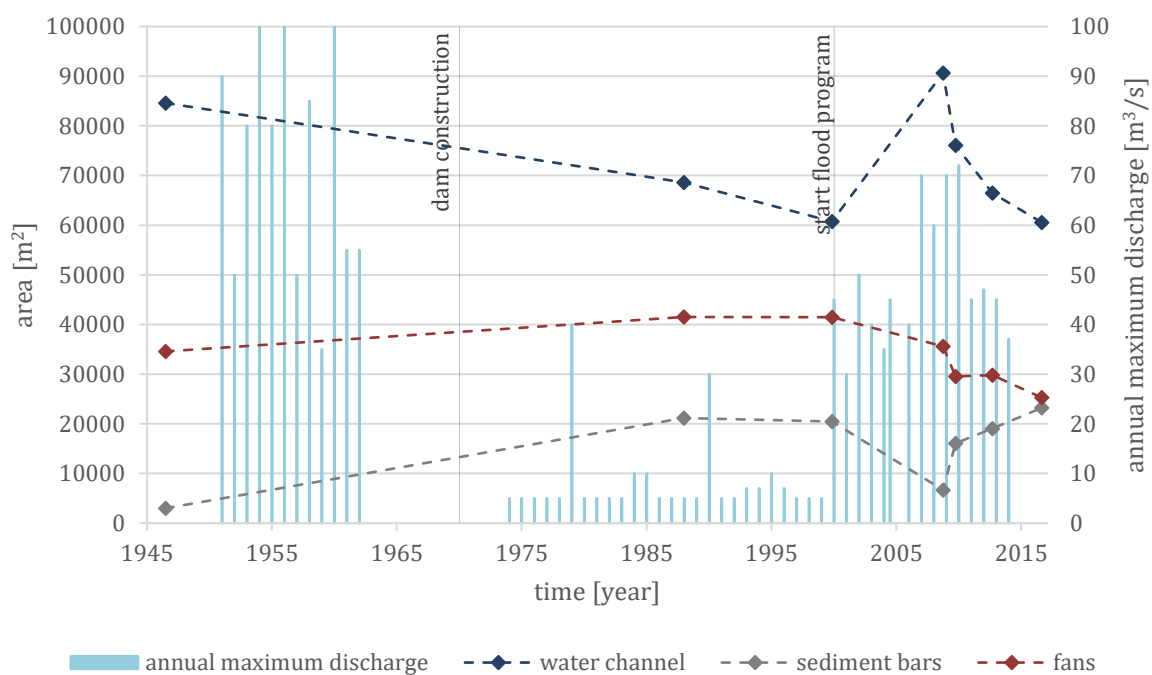


Figure 16: Area of the water channel, sediment bars and fans over time. The blue bars show the annual maximum discharge.

Results

Figure 17 shows the relative proportions of the main units in the whole mapping parameter. This includes the Total Active Channel (TAC) units, namely water channel, vegetated riparian units and sediment bars and, additionally, fan area from the surrounding floodplain units. The patterns are similar compared to the development of the absolute areas in Figure 16. Water channel decreases until 2000 and then slightly increases with an outstanding peak in 2009. Vegetated riparian units show a slightly increasing trend over the entire time span. Sediment bars show a minimum proportion in 1946 and 2009. Fan area slightly increased until 2000 and, from then on has shown a slight decrease.

Detailed observations of the development of one particular fan in the Spöl River are illustrated in Figure 18. In 1946 the talus cone of the fan was underdeveloped. The bend of the river is subsequently eroding the foot of the fan. In 1988 the fan propagated into the channel, developing a cone. In 2000 vegetation can be detected on the foot of the fan. From 2009 to 2017 the shape of the fan looks similar with some retreat compared to 2000. The vegetation has remained over these years.

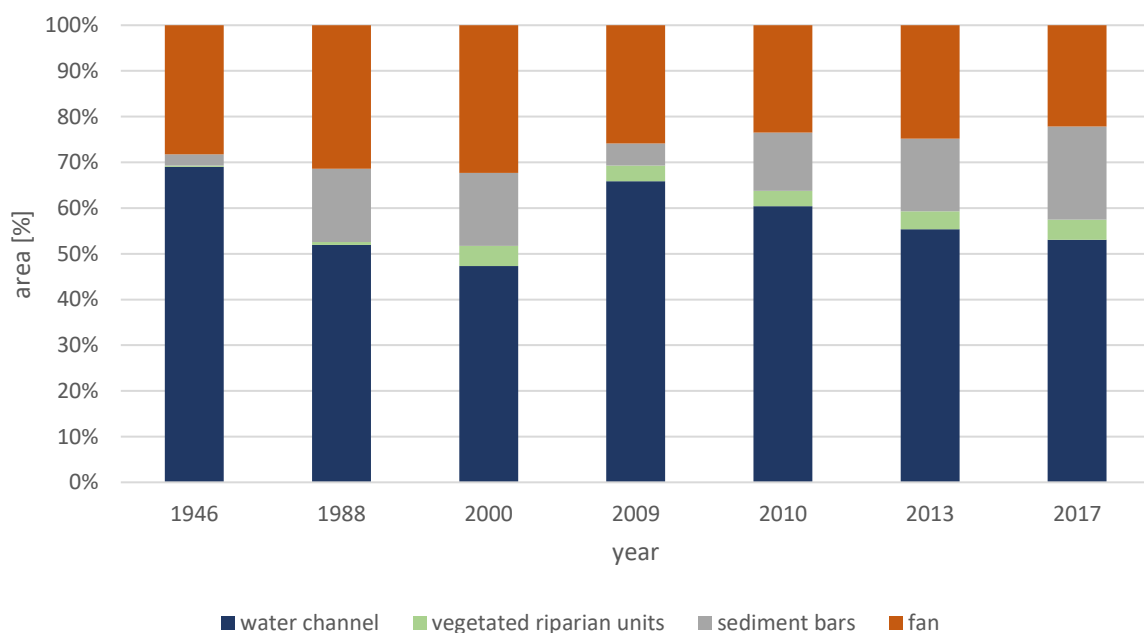


Figure 17: Relative proportions of the units forming the TAC in the considered years

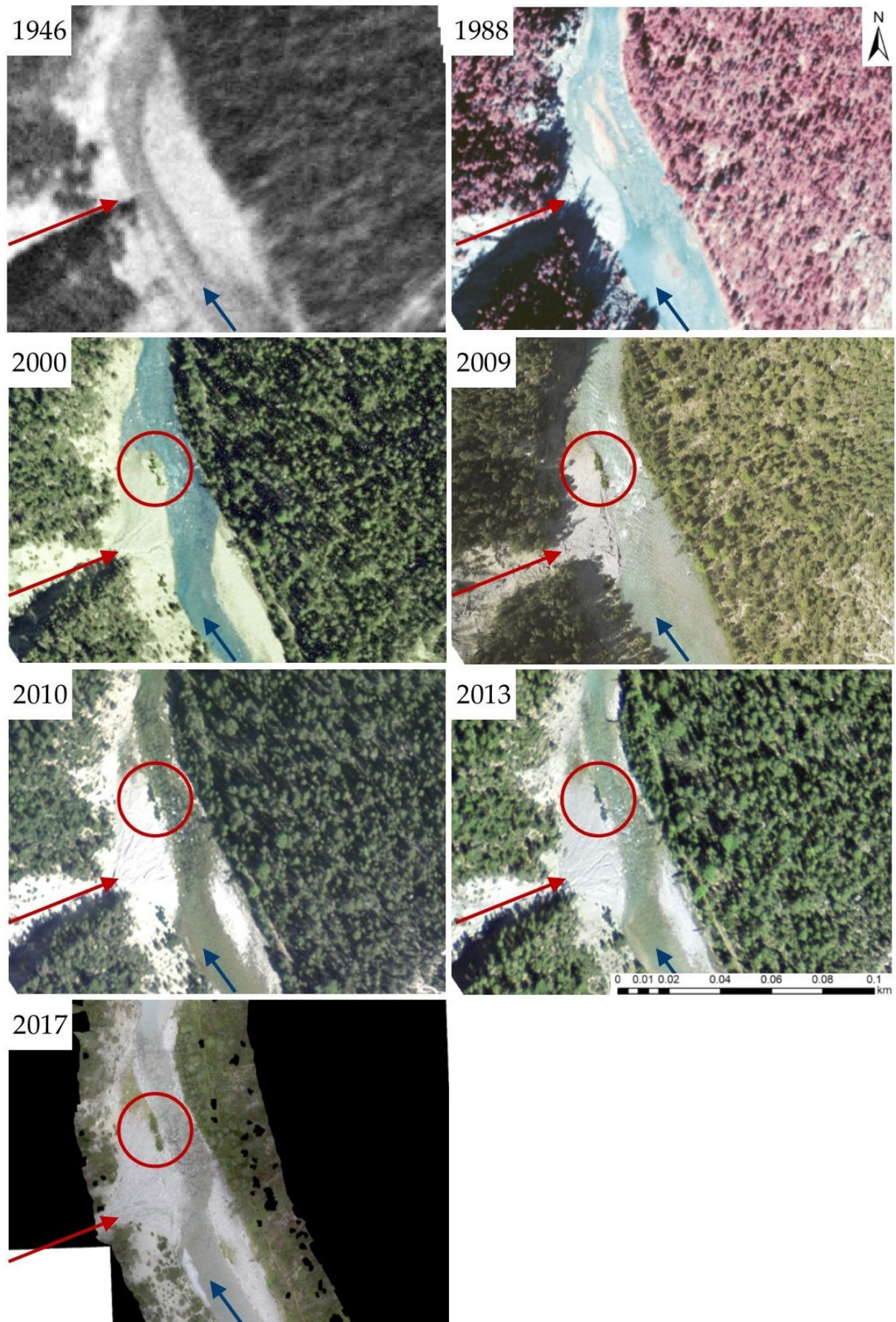


Figure 18: Development of a fan (indicated with a red arrow) from 1946 to 2017. The fan propagates into the active channel until the flood program gets started in 2000. From then the fan area slightly decreases, but the vegetated parts (red circle) remain vegetated. The blue arrow indicates flow direction.

Results

Figure 19 gives some more details about the proportions of the subunits amalgamated in the main units in Figure 17. In the water channel, riffles are the dominating unit in all years with a peak in 2009. An exception is the year 1946 where the water channel units could not be subdivided. The second largest unit is pool with a maximum proportion in 2000 and an increase from 2009 to 2017. The other units appear sporadically in small quantities. The sediment bars are subdivided into lateral bars (lb), mid-channel bars (mcb) and point bars (pb) where lb is the dominating group. The proportion of mcb is minimal in 2013. The proportion of pb shows a minimum in 2009 and a maximum in 2013. Vegetated areas are subdivided by density and site into densely-vegetated islands (DVI), sparsely-vegetated islands (SVI), riparian densely-vegetated (RDV) and riparian sparsely-vegetated units (RSV). The proportion of the subunits of vegetated areas vary a lot. In 1946 there are no vegetated islands, and dense vegetation is dominating on the banks. From 1988 sparse vegetation is dominating the vegetated areas and some islands appear sparsely-vegetated. Between 1988 and 2017, vegetation is densest in 2009 and lightest in 1988 and 2017.

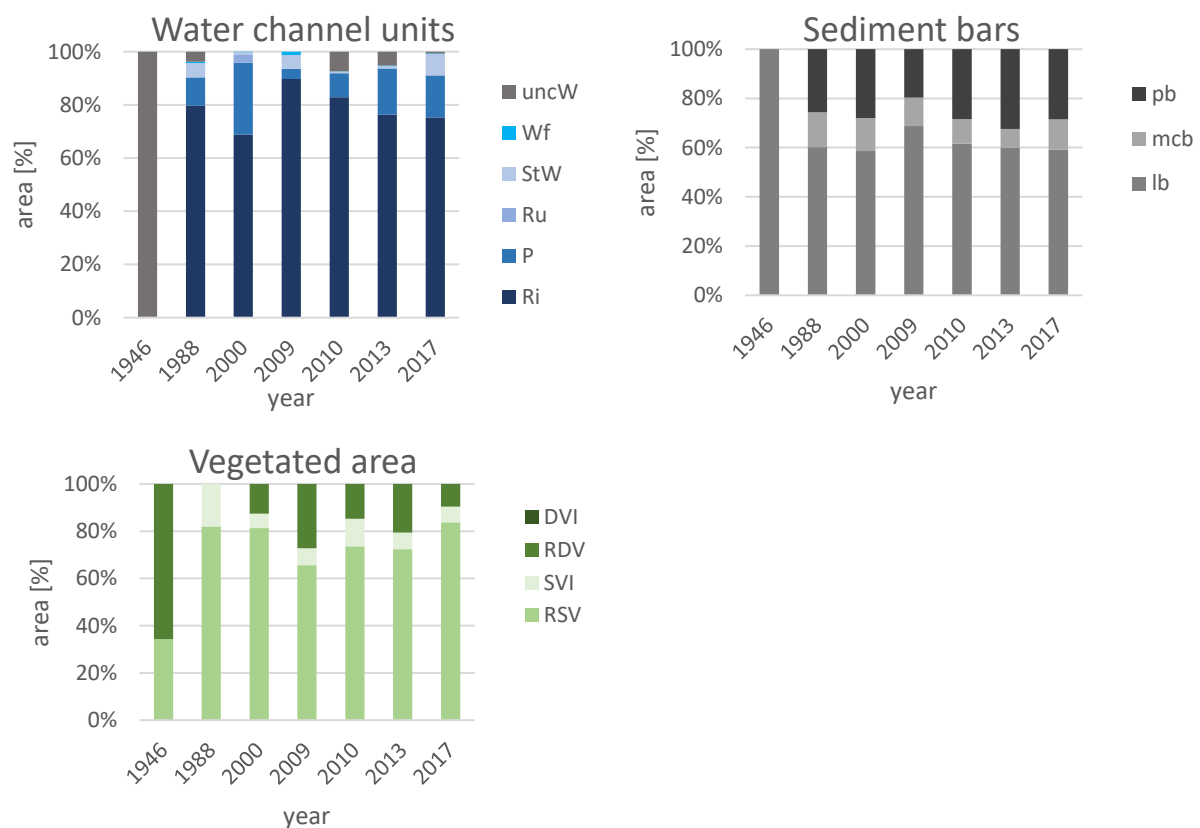


Figure 19: Relative proportions of the subunits forming the water channel (upper left), the sediment bars (upper right) and the vegetated areas (lower left). Classification code for Water channel units: uncW = unclassified water surface, Wf = Waterfall, StW = Standing Water, Ru = Run, P = Pool, Ri = Riffle; Classification code for Sediment bars: pb = point bar, mcb = mid-channel bar, lb = lateral bar; Classification code for Vegetated area: DVI = Densely-Vegetated units of Islands, RDV = Riparian Densely-Vegetated units, SVI = Sparsely-Vegetated units of Islands, RSV = Riparian Sparsely-Vegetated units

The channel width measurements are illustrated in Figure 20. The median width varies between 14 and 17 m with a minimum in 2000 and a peak in 2009. The maximum width was measured on the orthomosaic from 1946 with 35.5 m, minimum in 2017 with 2.2 m. The Kruskal-Wallis test indicates a statistically significant difference between 2000 and 2009. The differences between all other time sequential pairs are not significant.

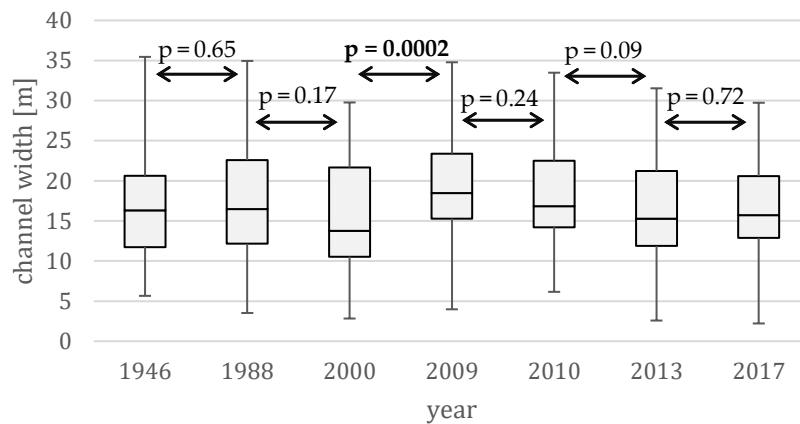


Figure 20: Channel width along the studied reach from 1946 to 2017. Results of the Kruskal-Wallis test for the significance of differences in the width between time sequential pair of years are also indicated. p values < 0.05 are indicated in bold.

Figure 21 shows a scatter plot of the width measurements made in the field and remotely with the help of the orthomosaics. The Spearman test indicates a statistically significant correlation between the two groups.

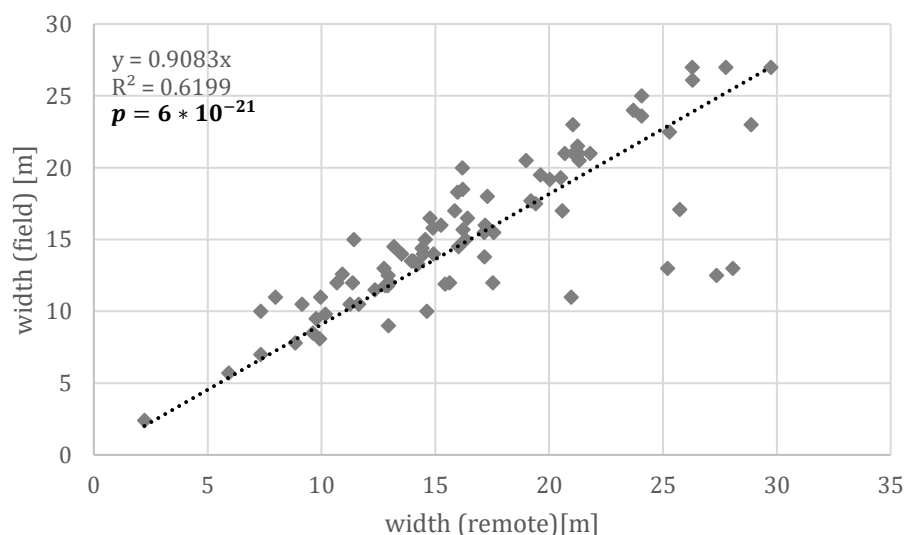


Figure 21: Comparison of width measurements in the field with remote width measurements on the orthomosaics in ArcGIS. The linear regression equation, as well as the coefficient of determination R^2 , are indicated. The p-value of the Spearman test indicates the significance of the correlation between field and remote measurements. p values < 0.05 are indicated in bold.

4.2 Sediment connectivity analysis

The results of the sediment connectivity analysis at catchment scale with the channel as a target are illustrated in Figure 22 (left). Some tributaries on the orographic right side in the upper part and on the left side in the lower part are medium to high connected to the Spöl River. But in general, the high connectivity is limited to the slopes confining the river bed. The tributaries Acqua and Foeglia coming from south-west show low connectivity except for the tributary channels which are medium to high connected to the outlet into the Spöl River. In the field evidence for high activity regarding sediment input was observed at the outlets of these two important tributaries. Considering the channels of the Acqua and Foeglia river in the connectivity analysis (Figure 22: right) the middle part of the tributary catchment is higher connected to the Spöl River. The higher elevated areas still appear as low connected. The fans, extracted from the orthomosaic from 2009, are entirely located in highly connected areas. Therefore, the fans are identified as important sediment sources.

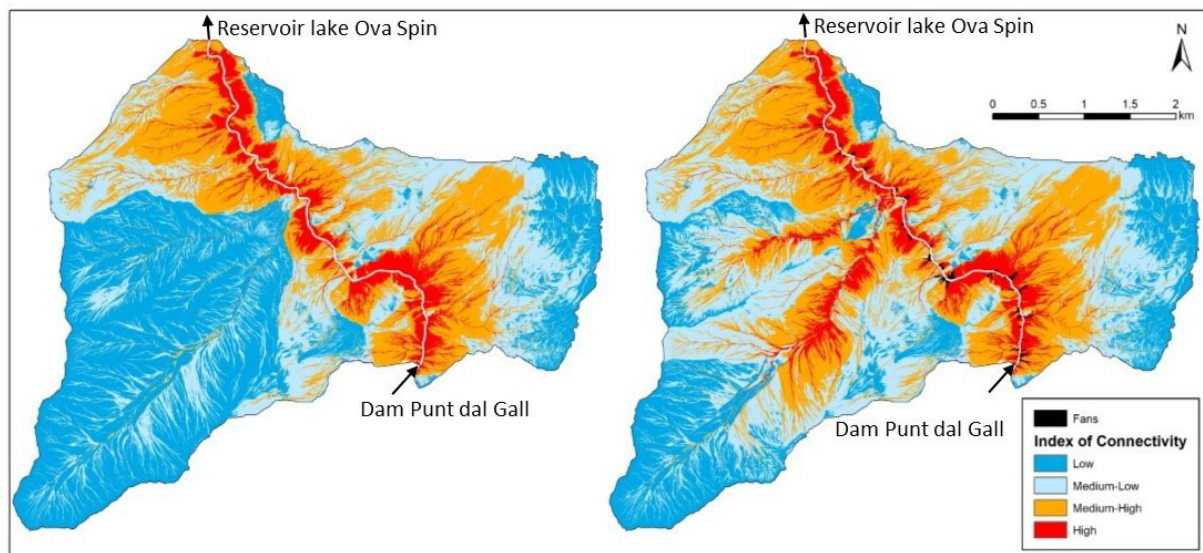


Figure 22: Classified map of the index of connectivity for the upper Spöl River with fans as sediment source areas. Left: Spöl River as a target. Right: including channels of the most important tributaries as a target, namely Acqua and Foeglia (in flow direction).

4.3 Grain size analysis

Figure 23 gives an overview of the Grain Size Distribution (GSD) samples along the river reach from this study (2017) and the results from Pfäffli (2013). The sample values for the grain diameters d_m and d_{90} with mean values for sample groups laying close together are plotted in a longitudinal profile with bars indicating fans and tributaries. Changes in the mean values sometimes coincide with the appearance of fans or tributaries like at 1000, 2000, 2800 and 4300 m from the dam.

Compared to the results of 2013 the grain diameters of 2017 are generally lower in the upper part and higher in the lower part of the Spöl River reach for both d_m and

d_{90} . The change in this trend appears between 2800 and 4500 m from the dam. It coincides with the Acqua and Foeglia river outlet at 2800 m from the dam. The two tributaries flow into the Spöl River close to each other and therefore appear as one bar in Figure 23. The Acqua and Foeglia river link a large catchment area to the Spöl River (Figure 22).

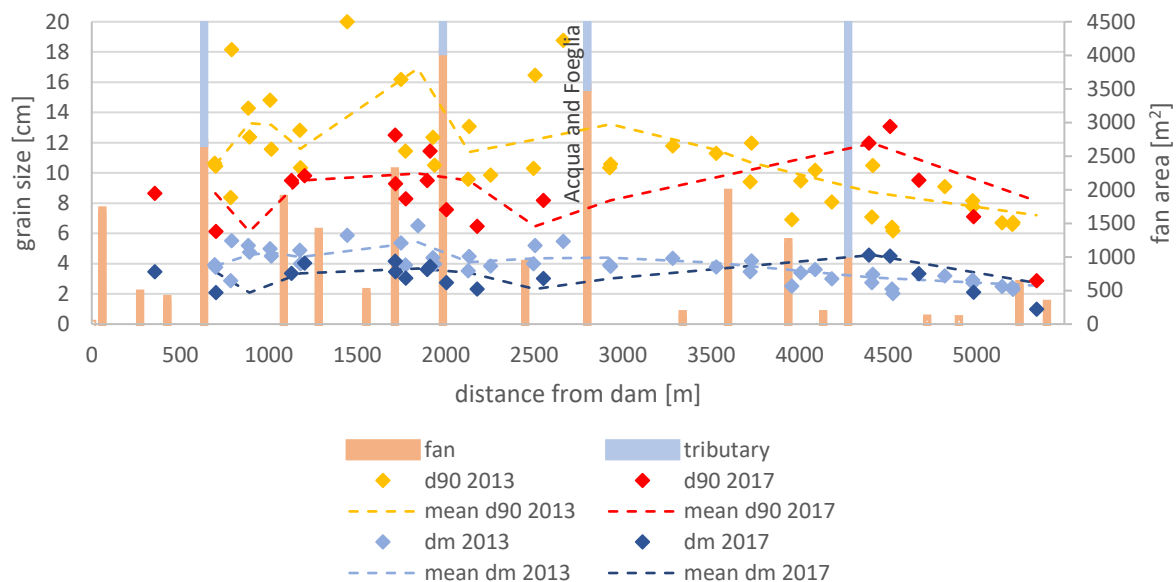


Figure 23: Overview of the GSD samples along the river reach. The points describe the characteristic grain diameter d_m and d_{90} of the samples from this study as well as the results from Pfäffli (2013). The dashed line illustrates the mean values from samples laying close together. Fans and tributaries are indicated with orange and blue bars, respectively. The main tributaries Acqua and Foeglia river are indicated as well.

Figure 24 shows the comparison of the two datasets from 2013 and 2017 for d_m and d_{90} , respectively. The Mann-Whitney test indicates a statistically significant difference in grain size diameters between the samples from 2013 and 2017.

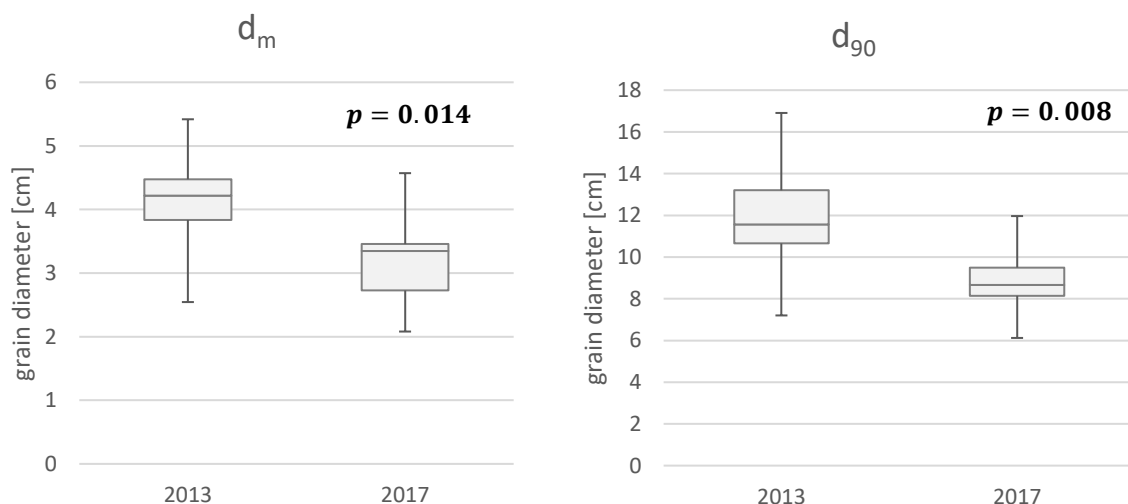


Figure 24: Grain diameter d_m and d_{90} of the samples from 2013 (Pfäffli, 2013) and this study (2017). Results of the Mann-Whitney test indicate the significance of the differences between the data sets. p values < 0.05 are indicated in bold.

4.4 High-resolution imagery survey

Figure 25 illustrates a section of the orthomosaic and the DSM generated using the drone Structure-from-Motion approach (SfM). The DSM is presented as a hillshade layer on which the orthomosaic is projected. The entire orthomosaic and DSM is found in the digital appendix (see page 62). Some details from the Agisoft Processing Report are listed in Table 5. The full report is part of the Appendix (page 62). The resolution for the orthomosaic and the DSM is 1.34 and 2.68 cm/pix, respectively. The location and error estimates of the 153 Ground Control Points (GCP) are given in Figure 26. Mainly the GCPs show small error estimates close to 0 m. At the GCPs p47 to p52 the error estimates rise to 2.4 m. The effect of this uncertainty on the orthomosaic and, consequently to the DSM, can be seen in Figure 27. The comparison of the original drone image (right) with the orthomosaic (left) exposes a doubling of the point bar in the narrow bend. A similar effect was found at the end of the studied reach. The GCPs Z01 to Z04 are remotely added and therefore lacking exact coordinates.

Figure 28 illustrates a section of the geomorphic map of the upper Spöl River. The section from Figure 25 is highlighted in Figure 28.

Table 5: Survey data from the Agisoft Processing Report (see Appendix)

	Orthomosaic	DSM
Number of images [-]	754	754
Coverage area [km ²]	0.364	0.364
Number of GCPs [-]	153	153
GCP error [pix]	1.2	1.2
Resolution [cm/pix]	1.34	2.68



Figure 25: Section of the orthomosaic and DSM generated using the drone Structure-from-Motion approach (SfM)

Results

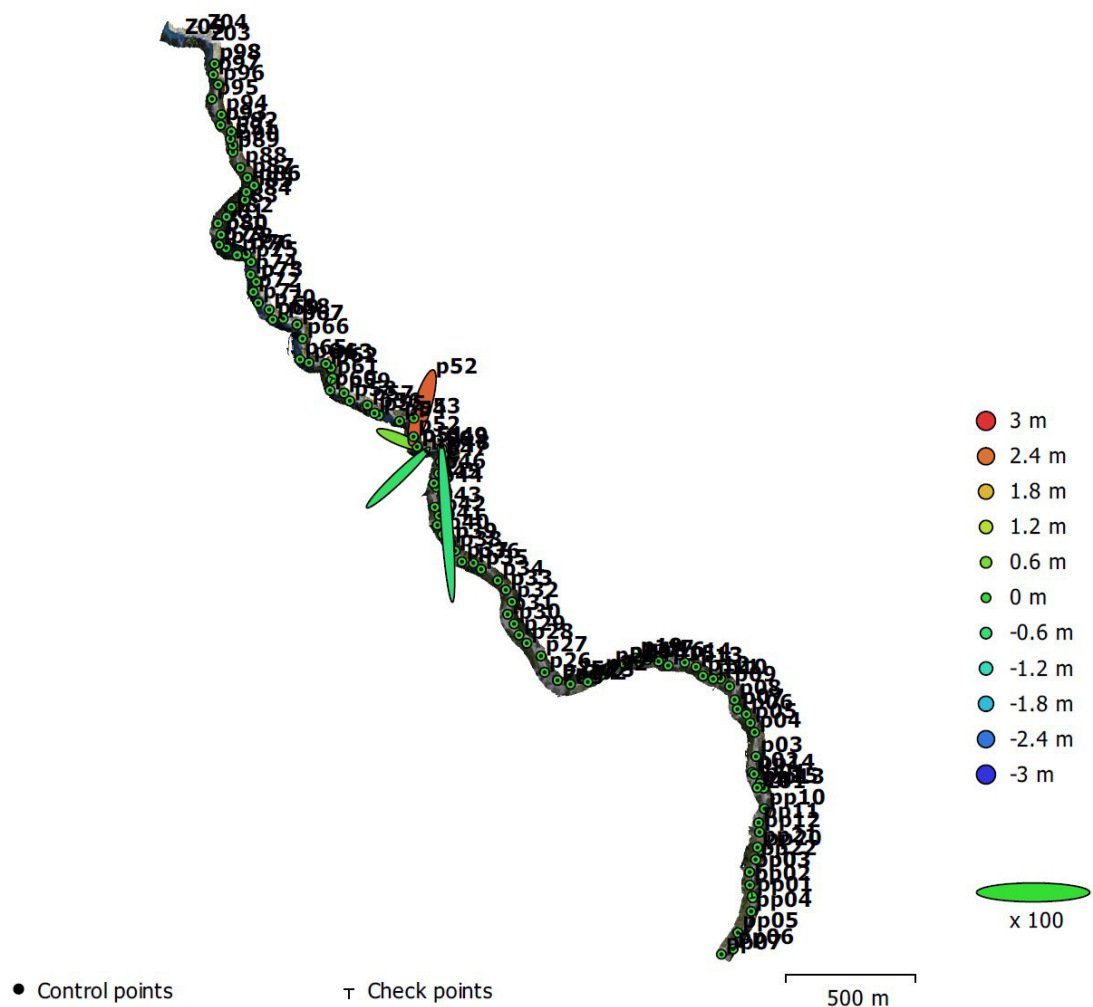


Figure 26: GCP location and error estimates from the Agisoft Processing Report (see Appendix)

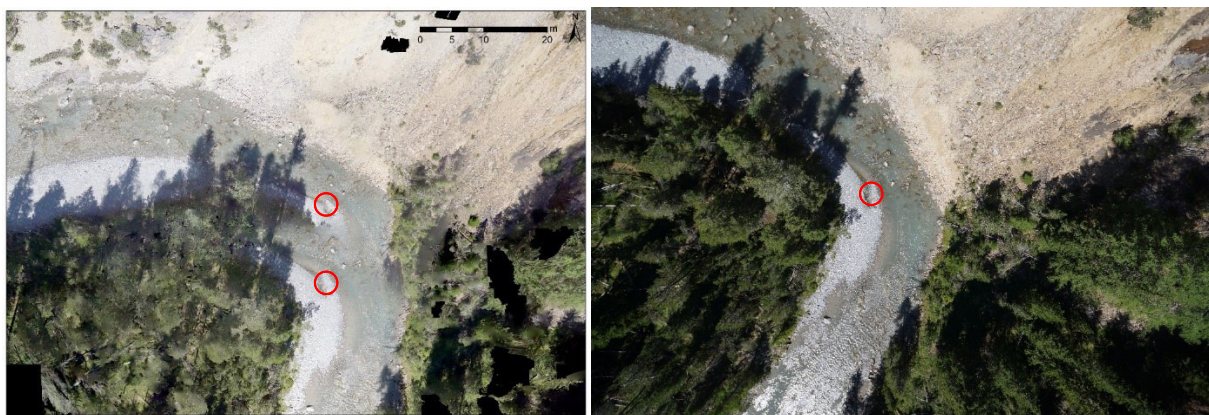


Figure 27: Orthomosaic section (left) and drone image (right) at GCP p48 (marked with a red circle)

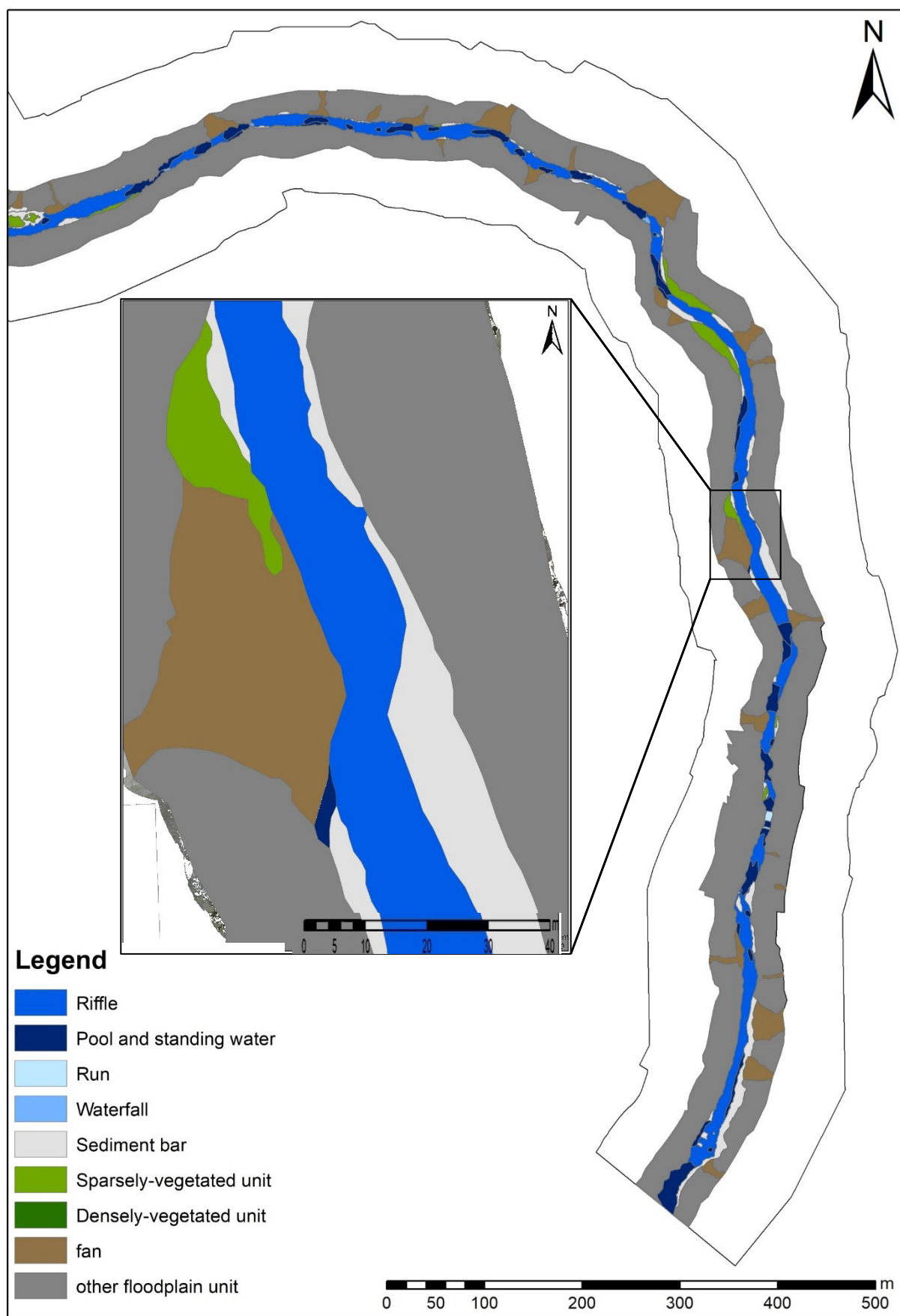


Figure 28: Geomorphologic map of the upper Spöl River

Results

The spatial distribution of the mapped geomorphic units is heterogeneous (Figure 29). For each subreach, the mean channel widths and channel slopes are calculated. Subreaches with a mean channel width larger than the total mean channel width are categorised as wide and otherwise as narrow (Figure 30). The same applies to the subreaches regarding their channel slope. Subreaches with a mean channel slope larger than the total mean channel slope are categorised as steep and otherwise as shallow (Figure 31). A third pairing is done regarding the two tributaries Acqua and Foeglia in the middle of the studied reach. They link the largest catchment area to the Spöl River (Figure 22). The studied reach is split at the outlet of the Acqua river, containing the subreaches 1-14 upstream the outlet of the Acqua river, referred to as “upstream Acqua” and 15-25 downstream, referred to as “downstream Acqua” (Figure 31).

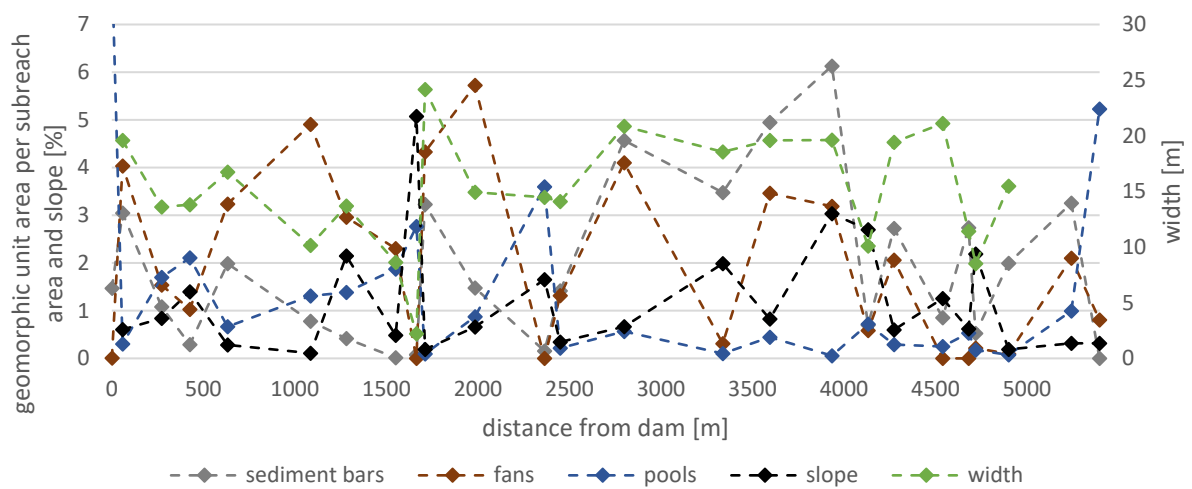


Figure 29: Overview of the heterogeneous spatial distribution of some selected geomorphic units along the studied reach of the upper Spöl River

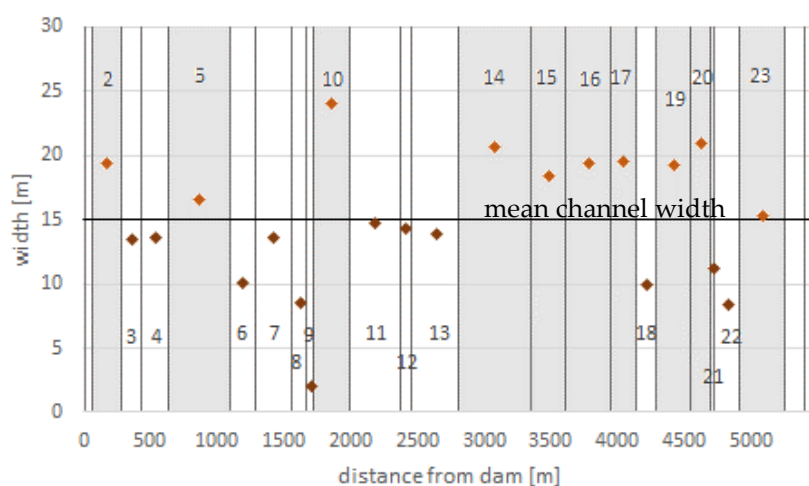


Figure 30: Subdivision of the studied reach into subreaches according to the channel width. Subreaches with a mean channel width > total mean channel width are classified as “wide” (grey background), the others are classified as “narrow”. Mean channel width is indicated with a black horizontal line.

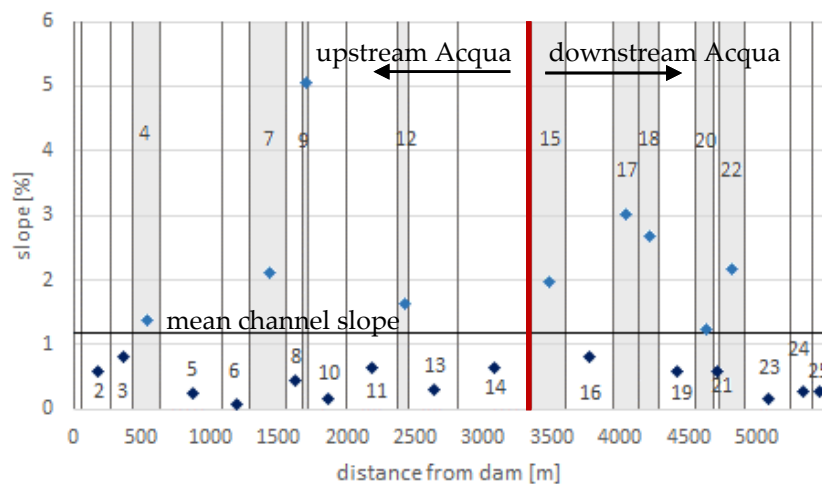


Figure 31: Subdivision of the studied reach into subreaches according to the channel slope. Subreaches with a mean channel slope > total mean channel slope are classified as “steep” (grey background), the others are classified as “shallow”. Mean channel slope is indicated with a black horizontal line. A red vertical line marks the splitting of the studied reach at the outlet of the Acqua river into upstream Acqua and downstream Acqua.

Comparing the mapped units regarding the width of the subreaches results in a statistically significant difference between wide and narrow reaches regarding sediment bar area, islands, pools, riffles, wood deposits, steps and bedrock appearance (Table 6). Range and mean values of the geomorphic units for wide and narrow subreaches, respectively, are illustrated in Figure 32. Sediment bar area proportions are larger in wide subreaches with a median proportion of 3.1% of the subreach area for wide and 0.6% for narrow subreaches. Riffles are mainly found in wide subreaches with a median proportion of 5.6% of the subreach area compared to 3.2% in narrow subreaches. In wide subreaches, the median wood count per meter length along the river is 0.06, and in narrow subreaches, it is 0.02 counts per meter length. Pool area proportions are larger in narrow subreaches with a median proportion of 1.3% of the subreach area for narrow and 0.3% for wide subreaches. Steps are only found in narrow subreaches without exception. In narrow subreaches, median bedrock length per meter along the river is 1.2 m/m. In wide subreaches, it is 0.2 m/m. Fan area and areas with standing water tend to be more represented in wide reaches and boulders and steeper slopes in narrow reaches but the differences are not significant. There is no difference in the width of the fans as well as in the confinement index between narrow and wide reaches. The mean confinement index for the entire upper Spöl River is 1.47 (Table 7).

Range and mean values of the geomorphic units for steep and shallow subreaches, respectively, are illustrated in Figure 33. Significant differences could only be found regarding the proportion of fan area per subreach area (Table 6). The proportion of fan area per subreach area is larger for shallow subreaches with 3.4% compared to 0.8% for steep subreaches. Sediment bars, riffles, standing water, steps, boulders and wider sections trend to be found in shallow subreaches. Pools and bedrock trend to be found in steep subreaches. But the differences between steep and shallow subreaches are not significant regarding the previously listed geomorphic units.

Results

Comparing the subreaches up- and downstream Acqua results in a significant difference in sediment bar area where more sediment area is found upstream Acqua (Table 6, Figure 34). The reach upstream Acqua trends to be steeper and narrower than the downstream Acqua but the differences are not significant.

Table 6: Results of the Kruskal-Wallis Test indicating the statistical significance of the difference of particular mapped units between the subreach type pairs (wide-narrow, steep-shallow, up- and downstream Acqua). p-values < 0.05 are highlighted in bold.

Mapping unit	p-value for width classes	p values for slope classes	p values for up- and downstream Acqua
slope	0.2914	-	0.3087
width	-	0.3673	0.1114
confinement index	0.6097	-	-
sediment bars	0.0005	0.0768	0.0004
fans	0.2752	0.0132	-
fan width	0.7409	-	-
pools	0.0024	0.6165	-
riffles	0.0010	0.1929	-
standing water	0.1868	0.1162	-
wood	0.0016	0.8152	-
steps	0.0053	0.9036	-
boulder	0.9474	0.2705	-
bedrock	0.0037	0.2167	-

Table 7: Range and mean values of the confinement index for wide and narrow subreaches and the entire studies reach

	wide subreaches	narrow subreaches	entire studied reach
Min	1.01	1.00	1.00
Mean	1.42	1.58	1.47
Max	3.65	4.51	4.51

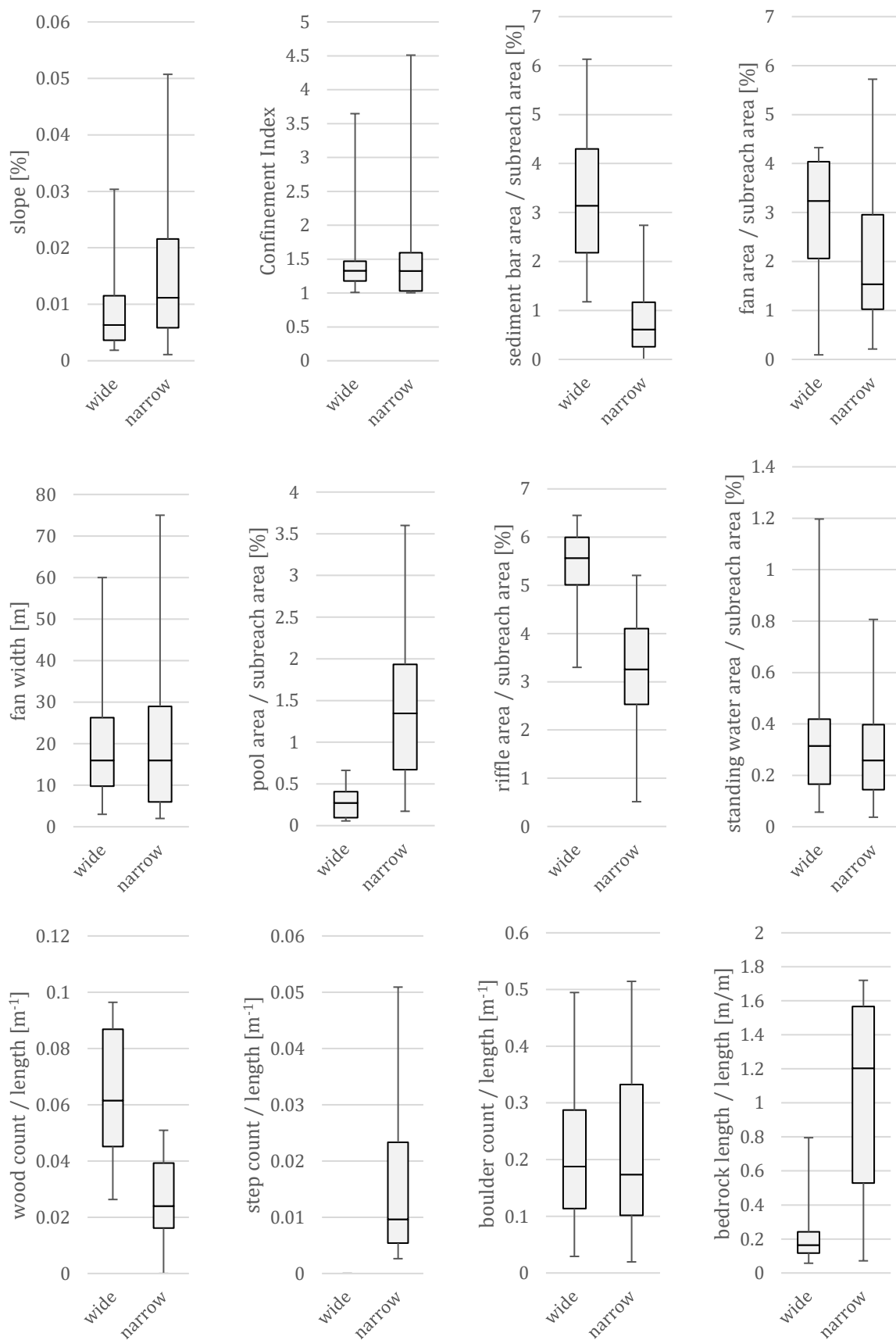


Figure 32: Range and mean values of mapped units along the Spöl River for wide and narrow subreaches. Subreaches with a mean channel width > total mean channel width are categorised as wide and otherwise as narrow (Figure 30). Statistical significance can be found in Table 6.

Results

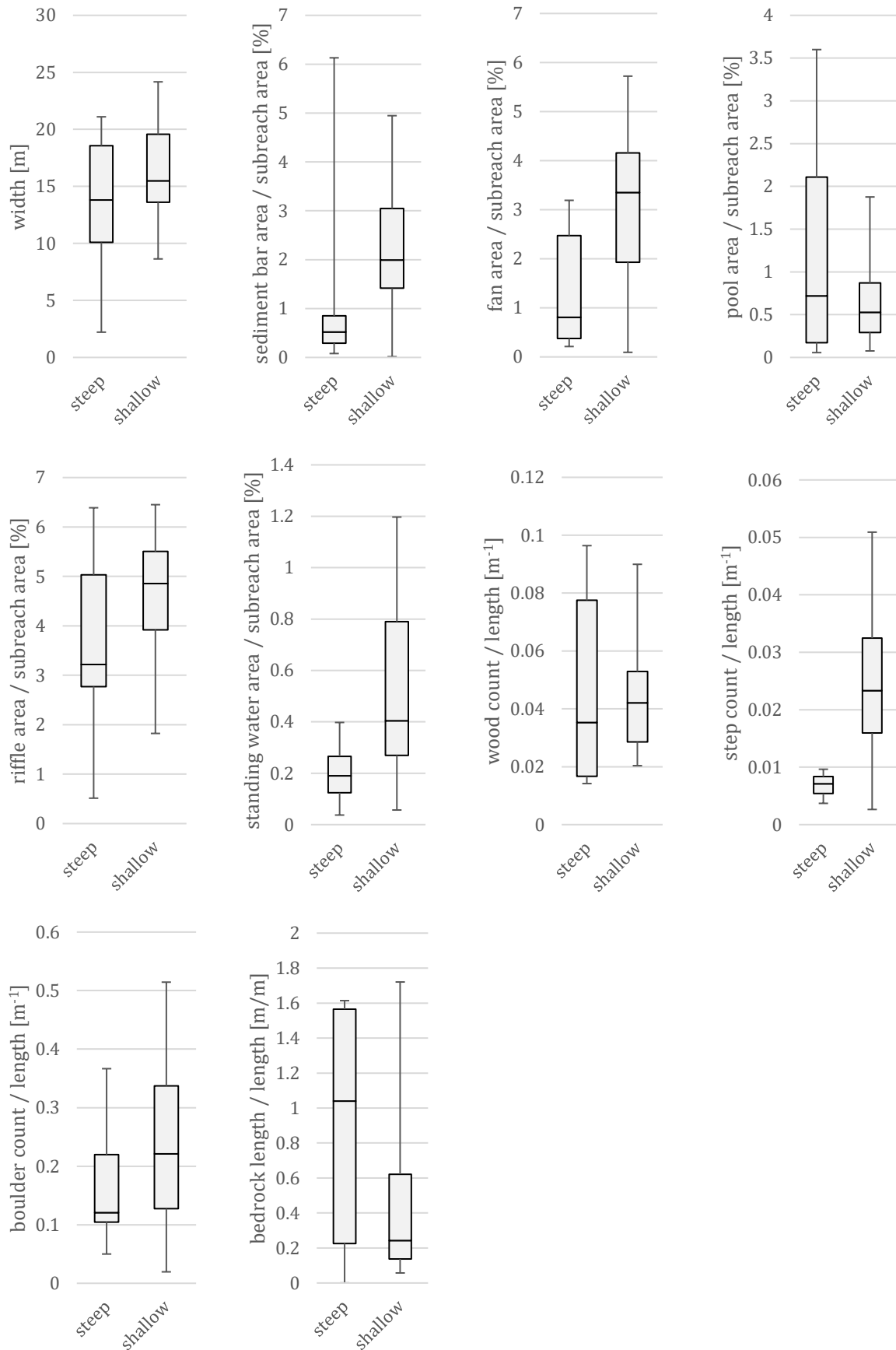


Figure 33: Range and mean values of mapped units along the Spöl River for steep and shallow subreaches. Subreaches with a mean channel slope > total mean channel slope are categorised as steep and otherwise as shallow (Figure 31). Statistical significance can be found in Table 6.

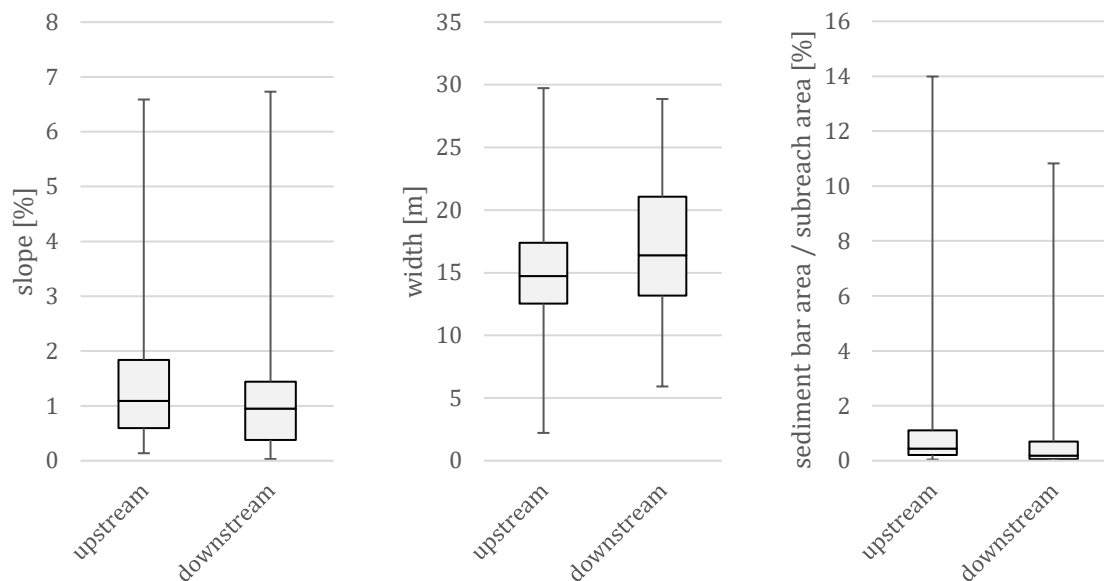


Figure 34: Range and mean values of mapped units along the Spöl River up- and downstream the outlet of the Acqua river, here referred to as “upstream” and “downstream”, respectively. Statistical significance can be found in Table 6.

Figure 35 shows the comparison of particular mapped units. The occurrence of sediment bars and fans is significantly correlated with each other. In the subreaches where fan area is larger, more and larger sediment bars appear. There is no significant correlation between the occurrence of fans and pools. The pool area ranges between 0 and 1000 m² per subreach with one outlier in subreach 25 with a pool area of 2000 m². Fan areas have a much larger range from 0 to 4000 m² per subreach. The Spearman test results in a significant correlation between boulder count and fan area as well as between wood count and fan area. High counts of boulders and wood are with high probability found in subreaches with larger fan area. Sediment bars and pools show no significant correlation. However, there is a slight decrease in pool area with increasing sediment bar area. The correlation between boulders and sediment bars is not significant. Generally, there is a slight increase in boulder count when having a larger sediment bar area. However, for wood and sediment bars there is a significant correlation. High counts of wood are with high probability found in subreaches with larger sediment bar area. Pools are neither significantly correlated to boulders nor wood. Generally, high counts of boulders as well as wood are found in subreaches with smaller pool area. Between the occurrence of boulders and wood, there is no significant correlation. There is a slight increase in boulder count with an increasing wood count. 240 wood logs were counted in the 5.5 km long reach of the upper Spöl River. With volume estimations after Wohl et al. (2010) this equals a volume of 30 m³ or 0.2 m³/km².

Results

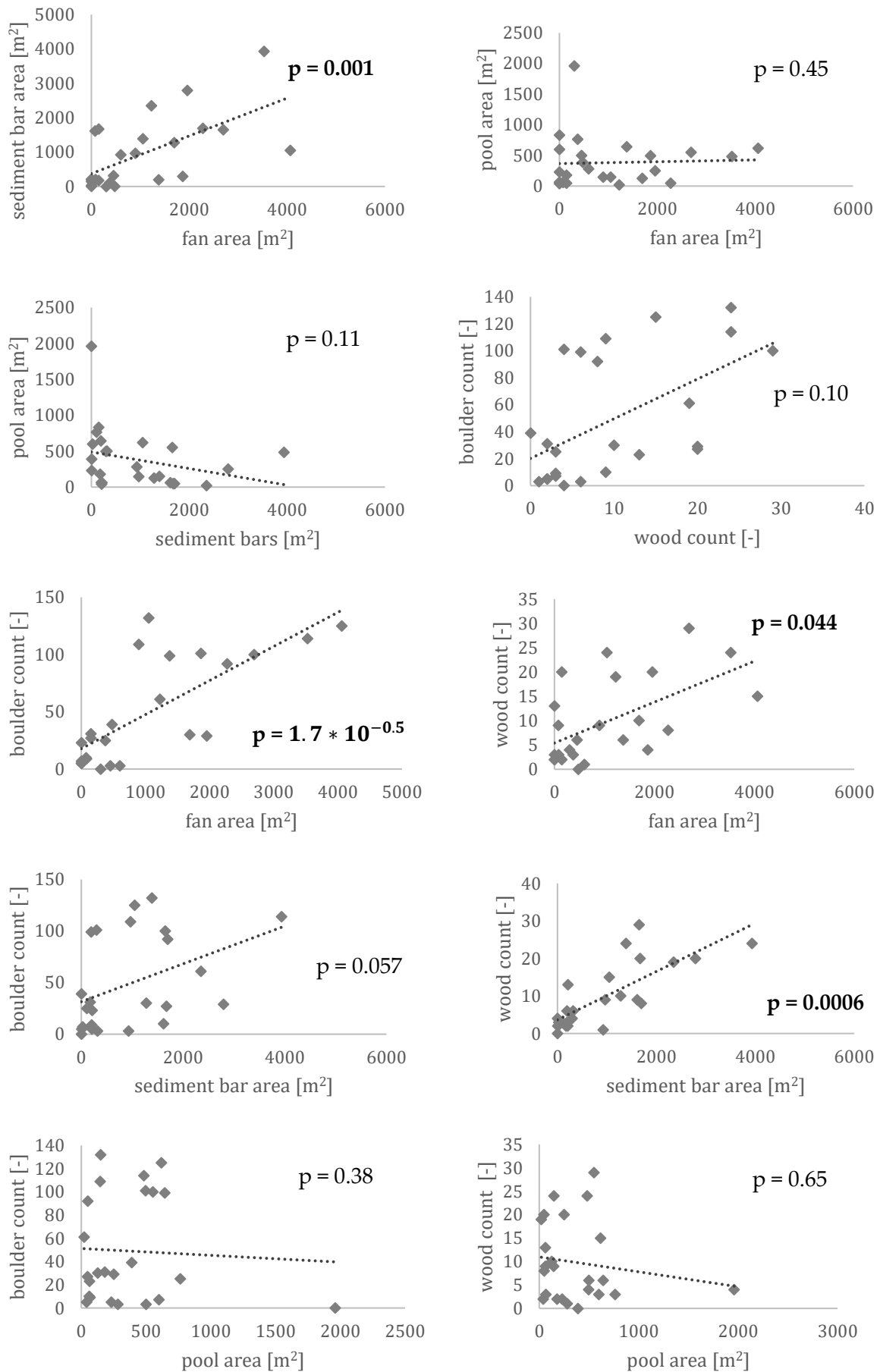


Figure 35: Comparison of particular mapped units. p-values < 0.05 are indicated in bold.

5 Discussion

The approach of this thesis contains a historical analysis, a sediment connectivity analysis, a grain size analysis and a high-resolution imagery survey. The advantages and limitations of the methods are discussed in the following section for each analysis, respectively. Then, a discussion of the derived results follows.

5.1 Methods

5.1.1 Historical analysis

Manually mapping geomorphic units on different orthomosaics is time-consuming and already includes interpretation in the acquisition of data. The orthomosaics are of different resolution and taken in different seasons with different flow rates what additionally increases the uncertainties (Table 2). There is a good qualitative concurrence of the validation measurements in the field with the remote mapping. The quantitative width measurements taken in the field, match well with the remotely measured channel width with a coefficient of determination (R^2) of 0.62 and a p-value of the Spearman test of $6 \cdot 10^{-21}$ (Figure 21). This match indicates that the remotely mapped units on the orthomosaic from 2017 are highly accurate. The orthomosaic from 2017 has the highest resolution and was taken during a low flow period in summer. These are the best conditions for remotely mapping on an orthomosaic (no snow cover, good detectability of geomorphic features due to low flow and high resolution). The other six orthomosaics were all taken during summer or early autumn, so there was no snow cover as well. But discharge highly varied, and on some orthomosaics, big areas are covered by shadow and are therefore undetectable. The resolution varies depending on the acquisition methods. The mapping on the orthomosaics from before 2000 have the largest uncertainties for they have the lowest resolution. On the orthomosaic from 2009, the resolution is high with 10×10 meters per pixel, but the discharge is high for the survey was carried out during an artificial flood (Figure 38 in the Appendix). All these differences are a source of major uncertainties. Hence, the historical analysis only serves to get an overview of the previous trends in the development of the river but not detailed insight into particular changes over time.

5.1.2 Sediment connectivity analysis

Originally, the connectivity index was developed for soil erosion studies (Borselli et al., 2008). Some adaptations made it suitable for alpine catchments, too. However, it does not consider processes like rock falls, rock- and snow-avalanches (Cavalli et al., 2013). Nevertheless, it is a good concept for a rapid spatial analysis of the potential connection between hillslopes and channel in an Alpine catchment (Cavalli et al., 2013).

The stand-alone application SedInConnect 2.4 opens the opportunity of a semi-quantitative estimate of sediment connectivity in a river catchment. It is user-friendly and requires only a few input parameters like a DEM and a target. The DEM from swissALTI3D from 2009 was the most recent DEM available and, with a grid size of 2×2 meters per pixel, it has a high resolution to get a first overview over the linkage

of sediment sources to the Spöl River. As proposed by Crema et al. (2015) the connectivity values are classified into four classes by the distribution of the connectivity values. The accuracy is limited to the resolution of the implemented DEM. With the roughness index derived from the DEM as weighting factor, the connectivity analysis is based on the DEM only. This simplifies the application of the tool. As a limitation, vegetation cover is not included. Vegetation can store sediment and therefore, limit connectivity (Puigdefabregas et al., 1999). The evaluated connectivity probably overestimates the forested parts of the catchment. In agreement with Cavalli et al. (2014) this aspect was neglected. According to Messenzehl et al. (2014), a combination of geomorphic field mapping and morphometric GIS modelling is essential to characterise sediment dynamics. With a detailed investigation and geomorphic mapping of the surrounding area of the Spöl River potential buffers could be identified and included in the connectivity analysis to improve the significance. There are GIS-based modelling approaches considering aspects like vegetation and different geomorphic processes to analyse sediment connectivity in more detail (Wichmann et al., 2009; Thiel et al., 2011).

5.1.3 Grain size analysis

With a process time of up to 4 images per hour, photogrammetry proved itself to be a simple and rapid method to gather grain size samples. The application with ImageJ is user-friendly and straightforward. According to Klein (1987), the principal advantages of photogrammetry can be found in the preservation of the image of the surface and the reduced effort in the field. According to Church et al. (1987) size measurements from photographs seem to be slightly smaller compared with field measurements (grid-by-number). They explain this difference with hiding effects and tilting of the grains so that the b-axis appear foreshortened. Other studies are dealing with the differences of field measurements and photogrammetry, highlighting different bias (e.g. Kellerhals and Bray, 1971; Adams, 1979; Ibbeken and Schleyer, 1986, Church et al., 1987). Kondolf et al. (2005) quote the measurement of grain axes from the photographic image to be the main source of error.

5.1.4 High-resolution imagery survey

As a rotary winged drone, the AscTec Falcon 8 needs small space to launch and land. This is essential in a narrow valley such as the one where the Spöl River flows through. The associated planning software AscTec Navigator is user-friendly. 24 flights could be planned in less than five hours. Nevertheless, the planned flights needed to be adapted in the field according to visual range and launch elevation. Including preparing the drone and adapting the flights one flight took about 30 to 45 minutes. The weather conditions during the high-resolution imagery survey were dry with moderate temperatures and slight cloud cover. Images gathered in twilight are unusable because of the weak lighting. Shadows and poor illumination are assumed to hinder the image matching process (Eltner et al., 2013). Hence, it is recommended to fly around noon where the shadows are shortest to improve lighting uniformity and therefore,

quality of the resulting model. The distribution of the Ground Control Points (GCP) in a zigzag line is important for the stability of the model. All GCP's were well visible on the images. It is important to fix the GCPs in places where they cannot be flushed away for at least some weeks. Replacing the lost GCPs with prominent points in the landscape worked well but it is not always easy to recover the exact points on the images, and consequently, model resolution suffers. The lack of ground reference close to the reservoir lake Ova Spin highly influenced the accuracy of the model in this section. In one section the GCP error estimates are up to 2.4 m. The reason for this error can be found in the shape of the river. In this section, the river follows a narrow bend. This leads to a broad spectrum of shooting angles in a minimal number of images. Additionally, two flights are overlapping in this section. To prevent such situations, narrow bends should be covered by one flight. In the case of the narrow bend in the Spöl River, this was not possible due to the limited visual range. The two flights overlapped with one waypoint. When two flights are needed to cover a bend, the overlap should include at least three waypoints or, respectively, 30 meters. An increased image density would also help to avoid angle gaps and doubling effects. Image density can be increased by increasing the minimal overlap of the images in the planning software. How high this overlap would need to be to reach sufficient image cover depends on the landscape and needs to be tested for example in test flights before starting the high-resolution survey.

Compared to classic digital photogrammetry the Structure-from-Motion (SfM) workflow is characterized by a much higher level of automation and much greater ease of use (Fonstad et al., 2013, Snavely et al., 2006, 2008, and Snavely 2008). The data processing is computationally demanding and time-consuming. The surveyed river reach comprises 754 images which cover an area of 0.4 km². It is a long reach compared to the surveyed river reach in Woodget et al. (2017) with 134 images covering an area of 8800 m². The image processing with Agisoft Photoscan Professional Edition 1.3.4 using an Intel Core 7i 32 GB RAM 64-bit computer took approximately one week, while Depth Maps and Dense Point Cloud Reconstruction was the most time-consuming processes with a process time of three to four hours each flight. To shorten the processing time the use of higher performance computing is needed.

Drone images capture only visible surfaces. As a constraint, the resulting model cannot reconstruct the features underlying vegetation, and steep walls appear blurred. Limited to vegetation cover, the elevation model tends to overestimate true elevation (Woodget et al., 2017). With the SfM approach water surfaces cannot be penetrated. Hence, the geomorphic mapping is limited to exposed features and the water surface (Buffington and Montgomery, 2005). Airborne bathymetric LiDAR (McKean and Isaak, 2009) or additional topographical survey in the field (e.g. GPS recording of cross-sections (Mürle, 2000)) would compensate for this limitation and enable reconstruction of subaqueous topography.

The orthomosaic and the DSM show some blurred parts and wholes, mainly at the borders of the model as a result of the angle of the camera lens. These border effects do not affect the model for the river, and its direct surroundings are not concerned. To minimise such effects, the flights should be done following a grid with at least two

lines parallel to the river. It is more time consuming and not practicable in narrow valleys. Errors within the SfM process are difficult to be found and isolated because of the black-box nature of Agisoft Photoscan Pro (Woodget et al., 2017).

The manual mapping method is discussed in 5.1.1 Historical analysis (page 41). There are tools for automatized classification of geomorphic units like the Geomorphic Unit Tool (GUT) (Bangen et al., 2017). Based on a 3-tiered hierarchical classification from Wheaton et al. (2015), the GUT is a powerful tool to distinguish geomorphic units and evaluate instream habitat conditions and development, especially regarding management activities (Kramer et al., 2017). For repetitive high-resolution imagery surveys along the upper Spöl River, it is highly recommended to test the application of such a tool in order to shorten process time and improve consistent classification and therefore comparability between the developed DSMs.

5.2 Results

5.2.1 Historical analysis

The observed changes in the main geomorphic units over time (Figure 16) might be influenced by the artefacts resulting from the differences between the orthomosaics (resolution, discharge). The peak in the water channel area, as well as the low peak in sediment bar area in 2009, is mainly due to the high discharge of the river on this orthomosaic for it was taken during an artificial flood (Figure 38 in the Appendix). The changes observed on the orthomosaics from 1946 to 1988 may have uncertainties due to the low resolution of the images. However, the general trends can be well explained by the development of the river due to the dam construction and the flood program. When the dam was constructed in 1970, the Spöl River remained as a residual stream with much smaller discharge than before dam construction (Scheurer and Molinari, 2003). This leads to a decrease in water channel area, and therefore, more sediment bars come to the surface. This is recognisable in the increasing sediment bar area from dam construction until the flood program gets started.

After dam construction, the natural high flows are missing as well and with it the moving forces for sediment transport (Mürle et al., 2003). The hypothesis that the fans expand after dam construction for they are not eroded anymore is supported by the slight increase in fan area from 1946 to 2000 (Figure 16). After the start of the flood program, the fan area slightly decreases. This observation matches with a previous assessment from Mürle et al. (2003), who documented a significant erosion of sediment at the foot of fans within the active channel during floods. After 17 years of artificial flooding, the retreat of fans stopped, and fans and active channel reached equilibrium. The observed stable positions of some large wood logs and boulders confirm the Spöl River as a transport-limited river system.

The subclassification of the water channel highly depends on the resolution of the orthomosaic and the flow regime. At the lowest resolution in 1946, different water channel units could not be distinguished. Therefore, the water channel area is unclassified. That the proportion of pool area in the water channel is largest in 2000

can be explained with the low and calm flow during the shooting and the previous 30 years with the Spöl River as a residual stream. The reduced flow dynamics lead to smooth water surface which is mapped as pool area. The variety increase in water channel units from 2009 to 2017 goes hand in hand with an increase in resolution. With higher resolution, the water channel appears differentiated and not only rough surface indicating riffles can be distinguished.

Lateral bars are the dominating sediment bar unit, and mid-channel bars show the smallest proportion. It can be explained by the high confinement of the upper Spöl River (see 5.2.4 High-resolution imagery survey, page 46), limiting the possibility of the water channel to branch. The valley has only a few bends. Therefore, the proportion of the point bars is small.

Regarding vegetation density, the sparsely vegetated units dominate in all years except in 1946. On the orthomosaic from 1946, sparse vegetation is difficult to be seen due to low resolution and the black and white colouring. From 1988 to 2009 the density increases and there is a bigger proportion of vegetated islands. This can be explained by the lack of big flood events.

Changes in the channel width over time are small due to the high confinement of the upper Spöl River with a mean confinement index of 1.47. Nevertheless, the minimum median width of 14 m in 2000 can be explained by the Spöl River being a residual stream for the previous 30 years. Due to low activity, fan area increased, and the active channel narrowed. From 2000 to 2017 the differences in channel width can mainly be explained by resolution differences and discharge on the orthomosaics.

The influences of the dam construction and the flood program on river dynamics are detectable with mapping geomorphic units on orthomosaics of different age.

5.2.2 Sediment connectivity analysis

The range of the index of connectivity (IC) of -8.5 to 3.3 is similar to the range determined by Messenzehl et al. (2014) in the study “Sediment connectivity in the high-alpine valley of Val Mütsch, Swiss National Park – linking geomorphic field mapping with geomorphometric modelling”. They analysed the sediment connectivity in the Val Mütsch, a catchment area next to the Spöl River. For the connectivity analysis, they used the same tool and a similar approach as applied in this study. Additionally, they mapped sediment storage and the potential (de)coupling in the field. For the connectivity analysis of the Spöl River, these aspects, as well as vegetation cover, are not taken into account.

The slopes confining the river bed are highly connected to the channel. Field observations confirm that these slopes are mainly covered by forest and debris fans. The sediment can be assumed to reach the river coming from the fans. Possible sediment sources in forested areas are held back by the trees. Because of the dam, the Spöl River does not receive sediment input from upstream. The fans can be interpreted as the main sediment sources for they are located in high connected areas. The catchment area of the tributaries Acqua and Foeglia is highly connected to their channels which

are highly connected to the Spöl River. To establish them as important sediment deliverers a detailed analysis of their catchment and their sediment dynamics is needed. The impact of the tributaries on the grain size distribution along the Spöl River is discussed in 5.2.3 Grain size analysis (page 46). How the tributaries affect the morphodynamics is discussed in 5.2.4 High-resolution imagery survey (page 46).

5.2.3 Grain size analysis

The measured mean grain size (d_m) of 3.2 cm is slightly smaller than the d_m of 3.9 cm determined in 2013 (Pfäffli, 2013) using a line-by-number analysis. The statistically significant difference between the two data sets can partially be explained by the different sampling methods. Grain sizes from photographic measurements tend to be smaller than field measurements (see page 41). An additional explanation for the differences is that we took a lower number of samples (17 samples) compared to Pfäffli (2013) (42 samples) and not in the same spots. But the differences can also be explained by the morphodynamics. In summer 2017 no artificial floods were implemented. The fine grains are not washed out as in years with floods leading to a decrease in d_m . Field observations of accumulation of a big amount of fine sediment in the river confirm this assumption. Uehlinger et al. (2003) observed an accumulation of fine sediment due to the low flow conditions before the start of the flood program (1970-2000) leading to a clogged riverbed. This impaired the natural reproduction of fish population (Ortlepp and Mürle, 2003). If the lack of floods in 2017 impacted fish population, was not investigated.

The increase in grain size in the lower part of the Spöl River compared to 2013 (Figure 23) can be explained by the input of coarse-grained sediment from tributaries and fans. The tributaries Acqua and Foeglia link a catchment area of 5 and 2 km² to the Spöl River, respectively. They enter the Spöl River where the change in the grain size along the Spöl River appears (Figure 22). Through the connectivity of the channels of the tributaries Acqua and Foeglia to the Spöl River, their catchment is highly connected, and the probability that sediment is brought to the outlet of the tributaries is high. The catchment area of these tributaries contains moraine material and dolomites in the upstream and downstream areas, respectively. To properly identify the effect of these tributaries on the grain size distribution along the river an enhanced assessment of grain size before and after the tributaries is needed as well as field observations in the catchment area to evaluate the sediment sources and their linkage to the channel. Other factors, such as other possible sediment inputs (smaller and less obvious than fans and tributaries), local flow conditions and the topography, influence the grain size distribution in a river.

5.2.4 High-resolution imagery survey

The resolution of the orthomosaic and the DSM with 0.01 and 0.03 m, respectively, is similar to the derived resolution of 0.01 m for the orthophoto and 0.02 m for the DEM in the case study of Woodget et al. (2017). They used similar methods to cover an area of 3400 m², hundred times smaller than the covered 364000 m² in this study. Thanks to

the low discharge during the high-resolution imagery survey the geomorphic units are well detectable in most parts of the studied reach except for the section from GCP p47 to p52 where a mismatch occurs due to a narrow bend of the river.

The main difference between narrow and wide subreaches is the channel cross-section size which influences the hydraulics (Brierley and Fryirs, 2005). In wide subreaches flow velocity and water depth decrease, flow has lower power, and sediment deposition occurs (Brierley and Fryirs, 2005). Sediment areas and wood deposits are significantly more frequent in wide subreaches of the Spöl River. Riffles are commonly observed between bars (Brierley and Fryirs, 2005). We also found significantly more riffles together with bars in wide subreaches. According to Montgomery and Buffington (1997), pools, steps and bedrock exposure are correlated with narrow, steep channels. This could be confirmed to be the case for the upper Spöl River. The Spöl River is a high confined river with a mean confinement index < 1.5 (Gurnell et al., 2014). The differences in confinement do not allow a classification in confined and unconfined but rather in very high confined and high confined where the boundaries are less sharp and difficult to distinguish.

Obstacles like bars and wood can stow water. Hence, wood and sediment bars are significantly more frequent in wide subreaches, standing water is expected to be found there as well. Wood is confirmed to be transported through narrow reaches and retained in wide reaches (Wyzga et al., 2015). However, the difference between wide and narrow subreaches is not significant for standing water. There is only little data for standing water areas which could be an explanation for the lack of a clear trend. Regarding boulders, there is no significant difference between wide and narrow subreaches. The boulders seem to be regularly distributed with one boulder every 2 - 10 meters. Fan area is slightly larger in wide reaches. It can be explained by the limited space for debris cones and the steep valley slope observed in the field in narrow reaches. However, a significant difference in fan width, as well as the confinement index between narrow and wide subreaches, were not observed.

Steep and shallow subreaches only differ significantly regarding the fan area. The big fans in the shallow subreaches can have several explanations. On the one hand, shallow subreaches are supposed to be wider, and hence, the debris fans can develop bigger cones. However, a significant difference in channel width between steep and shallow subreaches was not found. On the other hand, fans deliver sediment to the river. A higher sediment supply can trigger a decrease in stream gradient (Buffington and Montgomery, 2005). This could not be attested in this study. Indeed, sediment bar area is larger in shallow subreaches, but the difference is not significant. Steps are observed to appear in steep channels (Montgomery and Buffington, 1997). However, they appear more often in shallow subreaches of the upper Spöl River though without statistical significance. There is only a small number of steps in the studied reach. Hence, this result is not conclusive. It is common to find riffles, standing water, wood deposits and boulders in shallow subreaches. However, significant differences between steep and shallow subreaches could not be attested. Pools are more frequently found in steep

subreaches. It can be explained by the flow energy. Flow energy is higher in steep subreaches, and turbulent flow forms erosional depressions resulting in pools (Brierley and Fryirs, 2005). However, the difference in pool area between steep and shallow subreaches is not significant in the studied reach.

Comparing the distribution of the geomorphic units up- and downstream the tributaries Acqua and Foeglia helps to explain the change in grain size before and after the input of the tributaries. Width, slope and sediment bar area were assumed as important criteria to show if the tributaries deliver a big amount of sediment to the Spöl River. If so, the downstream reach should be wider, shallower and contain more sediment deposits than the upstream reach (Buffington and Montgomery, 2005). Indeed, the lower subreach appears to be wider and shallower than the upper one, but differences are not significant. Sediment supply is not the only criterion for widening and shallowing of a river. Basin conditions like topography and streamflow are influencing channel characteristics as well (Buffington, 2012). Sediment bar area is significantly larger upstream the tributaries Acqua and Foeglia. This does not contradict the hypothesis that the tributaries deliver a significant amount of sediment to the Spöl River. However, the tributaries Acqua and Foeglia could not be emphasised as important sediment sources by comparing sediment bar area.

The significant correlation between fan and sediment bar area supports the assumption that debris fans are important sediment sources in the Spöl River. The count of boulders as well as wood deposits is also significantly correlated with the fan area. Therefore, fans can be interpreted not only as important sediment sources but also as deliverers of bigger obstacles. Another explanation for the correlation could be that fans are more likely in those subreaches where topography forces deposition. What the fans deliver is linked to the characteristics of their catchment area. These issues were not examined in this study and further investigations are needed to understand the spatial distribution of the sources of big obstacles like wood logs and boulders and the transport mechanism during floods.

Pool area is not significantly correlated with fan area, sediment bar area, boulder count and wood count. Brierley and Fryirs (2005) assumed fans and sediment bars to stow water and implement pool formation. Wohl and Scott (2016) could show a correlation between pools and obstacles like wood and boulders. None of these processes could be attested here. Hence, channel width is interpreted to be the main criterion for pool formation in the upper Spöl River.

We hypothesised that sediment bars are forced to form downstream obstacles like wood and boulders (Keller et al., 1995). Regarding wood, this hypothesis is supported by the statistically significant correlation of wood count and sediment bar area (Figure 35). Regarding boulders, the correlation is not significant. Wohl and Scott (2016) state that increasing wood volume increases sediment volume up to a threshold sediment volume. In the Spöl River large wood is not transported during the controlled floods (see 5.2.1 Historical analysis, page 44). This strengthens the hypothesis of the linkage of wood and sediment storage. Nevertheless, the deposition of large

wood, as well as boulders, can also be induced by sediment bar areas. Wood, as well as sediment deposition, is mainly controlled by hydraulic parameters like discharge, flow area and width and mean depth (Wyzga et al., 2015). Hence, channel width can be interpreted as the main criterion for sediment, wood and boulder deposition in the upper Spöl River. According to Abbe and Montgomery (2003) large wood mainly deposits on irregularities like boulders. This statement cannot be promoted with the distribution of wood and boulders in the Spöl River. There can be several reasons for the weak correlation between boulders and wood. On the one hand, wood input is limited due to the cut-off from the upstream input area through the dam and due to the reduced erosional power of the controlled floods compared to rivers with similar width and slope (Wohl and Scott, 2016). Jochner et al. (2015) indicate a similar amount of wood in the Erlenbach with a catchment area of 0.7 km², much smaller than the 185 km² of the upper Spöl River. On the other hand, the deposition site of wood and boulders varies depending on many other parameters like stream flow, water depth and channel width (Ruiz-Villanueva et al., 2016). The dominating parameter for both boulders and wood deposition was not examined in this study. Further investigations are needed to understand the depositional processes as well as the influence of the floods on the transport of bigger obstacles.

With the findings of this study, a conceptual model of the upper Spöl River is developed (Figure 36). The channel width, as well as the confinement, are understood as the main controlling parameters regarding the distribution of geomorphic units. Therefore, the model shows the characteristic differences of wide and narrow subreaches. The narrow subreaches are mainly incised in bedrock and, therefore, they are more confined. They are steep, and the water is deeper than in wide subreaches. Pools form mainly in narrow subreaches, some of them forced by boulder or bedrock steps. Fine sediment is accumulated in the pools in the narrow subreaches. Fans deliver sediment, boulders and wood, which are mainly transported through the narrow subreaches and deposited in the wide ones. The fans in the wide subreaches are wider and have larger areas than the fans found in the narrow ones. Grain size decreases from one fan until the next fan occurs, while pebble roundness increases. The wide subreaches are defined by depositional processes. Sediment bars and islands form in wide subreaches, partly forced through boulders or wood jams and partly due to hydraulic parameters. Vegetation is mainly found in wide subreaches. The vegetation density increases in flow direction. Floods rework vegetation patches and influence their density pattern (Mikus et al., 2013; Surian et al., 2015; Hajdukiewicz et al., 2016). The vegetation density distribution points to the impact of the artificial floods on vegetation in wide subreaches.

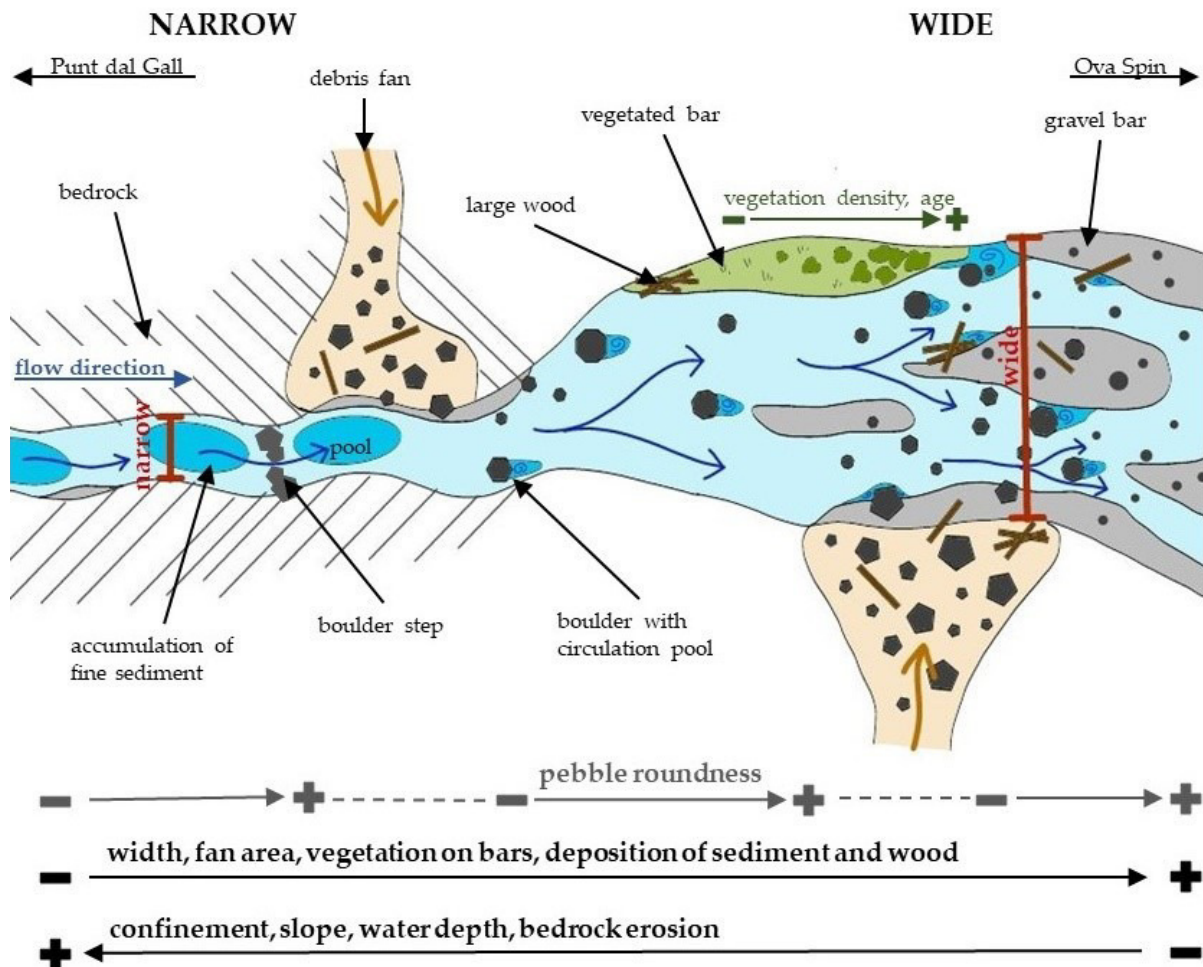


Figure 36: Conceptual model of the upper Spöl River showing the characteristics of wide and narrow subreaches

5.3 Implications for flood management and river restoration

Unmanned aerial survey and remote sensing are widely spreading in the field of geomorphology. Drones and digital photogrammetry have the advantage of making "question-driven, high-resolution research considerably more feasible than it has been previously" (Hervouet et al., 2011). In this study, we could show that the application of drones and photogrammetry are appropriate regarding geomorphic classification of a river. One has to mind challenges like the limited spatial coverage, large data volumes and the need for field validation (Woodget et al., 2017). Despite these current limitations, the application is beneficial for flood management and river restoration as it allows a consistent iteration of the acquisition of spatially continuous data. Changes in topography and distribution of geomorphic units can be detected by comparing data from two flights. To simplify and accelerate the classification process and guarantee comparability between iterations, the development of automatized classification tools is promising. The Geomorphic Unit Tool (GUT) (Bangen et al., 2017) is based on the geomorphic classification from Wheaton et al. (2015). The tool is developed to derive units from topography and information about bankfull and low flow channel (centerline and thalweg). It was designed to process DEMs created from total station

surveys of wadeable stream reaches with 10 cm resolution. There are further developments needed to use this tool with high-resolution DSMs derived from unmanned aerial surveys with 3 cm resolution.

The results of this study might be useful for the Swiss National Park in various ways. During remediation work at the outlet of the dam Punt dal Gall in 2016 a hazardous building substance was accidentally released into the Spöl River (press release, Standeskanzlei Graubünden, 22.12.2016). Elevated levels of PolyChlorinated Biphenyls (PCB) in fine sediments, fish and algae were detected in the upper Spöl River (press release, Standeskanzlei Graubünden, 22.12.2016). The rehabilitation actions are not clear yet (press release, Swiss National Park, 15.03.2018). The PCB was released in the form of dust (press release, Cantonal Police Force Graubünden, 04.11.2016). Therefore, it is assumed to accumulate in fine sediment. In narrow and deep sections accumulations of fine sediment were observed in the field. The geomorphic map can help the competent authority to identify possible sites of elevated pollution.

Robinson and Uehlinger (2006) showed that the river ecosystem of the Spöl River underwent a regime shift in the first three years of the artificial flood program. In the fourth year, a new or alternate ecosystem state was reached. They suppose that the river ecosystem still is in a state of hysteresis (as defined by Scheffer et al., 2001). Whether a new alternate state is reached can be tracked by observing ecological thresholds. The understanding of ecological thresholds is essential to perform adapted management strategies (Groffman et al., 2006). Hence, it is of great importance to engage geomorphic units with habitats. A habitat describes the physical surroundings of plants and animals (Jowett, 1997). The assessment of habitats in and along a river can help to evaluate river health “since it provides the natural link between the physical environment and its inhabitants” (Grove, 1999). Geomorphology is a key variable influencing a habitat (Figure 37). A first level classification can be done with a detailed geomorphic map as proposed by Rey and Hesselschwerdt (2017). They propose a method to link geomorphic units to habitats and to classify and assess them remotely for evaluating river health. They assume habitats to indicate the potential population of key species. According to them, good quality of water population goes in line with the presence of specific habitat types (Eberstaller et al., 2014; Rey and Hesselschwerdt, 2016). Based on the geomorphic map developed in this study a similar approach could be adopted to investigate river health for the Spöl River and to observe the ongoing ecosystem regime shift. Therefore, repeated unmanned aerial surveys should be implemented, and geomorphic maps should be developed using a consistent classification. The resulting geomorphic maps can be compared with the map provided in this study. This will improve the understanding of the spatial and temporal dynamics of physical habitats and, therefore, river health (Grove, 1999). The gained knowledge can be incorporated into the management strategies of the artificial flood program.

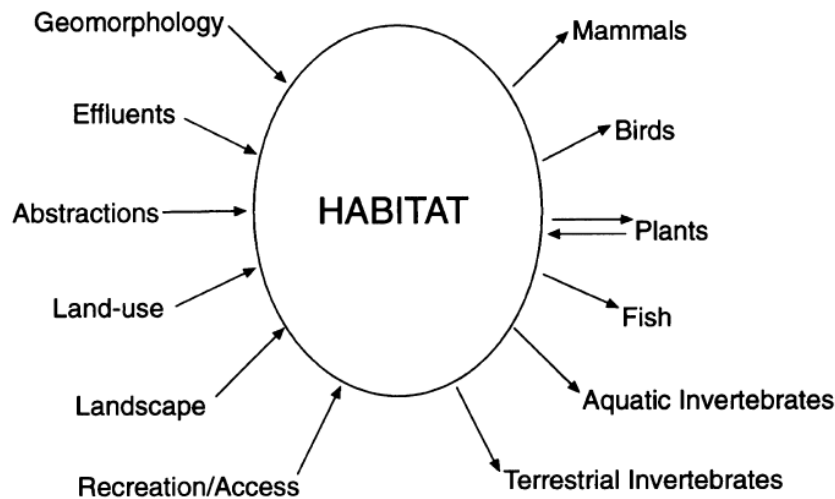


Figure 37: Concept of habitat as the natural link between the physical environment and its inhabitants (Harper et al., 1995)

Linking the geomorphic map to habitats makes it suitable for biologic and ecologic monitoring. Field survey is needed to investigate the defined habitats in more detail regarding indicators like aquatic plants and key inhabitants. The geomorphic map can help to define the approach and the key sites.

The geomorphic map developed in this study serves as a base for long-term monitoring of fluvial morphology and related processes in the Spöl River (Parkforschung, 01.04.2017). This project aims to identify, classify and map the main fluvial landforms along the Spöl River in a first phase. In a second phase, geomorphic changes after artificial floods will be analysed. This study is incorporated into the first phase, and repeated high-resolution imagery survey will be compared to the results pointed out in this study. An in-depth understanding of the geomorphic processes in the Spöl River during the artificial floods will allow predictions of geomorphic changes and deepen the understanding of the morphodynamic response or river systems to flow regulation.

6 Conclusions

This study combines field and laboratory investigations to characterise the morphodynamics in the upper Spöl River in the Swiss National Park. Despite the limitations of the historical analysis due to the different resolution of the orthomosaics, the management impact on the geomorphology could be shown. The dam construction led to a reduction in sediment dynamics in the Spöl River, confirmed by increasing fan area. With the implementation of the artificial floods, river morphodynamics was revived. The floods eroded the fans and flushed out the fine sediment fraction. That is how they prevented the riverbed from clogging with fines and from being repressed by the propagating fans. Due to a lack of floods in 2017, fine sediment accumulated in the channel. The mean grain size decreased compared to previous studies. To maintain the regained mountain river character, it is, therefore, crucial to take up the frequent flooding of the upper Spöl River as soon as possible.

The sediment connectivity analysis highlights the fans and the tributaries Acqua and Foeglia as the main sediment sources for the upper Spöl River. Their influence is mirrored in increasing steps in the mean grain size along the river. However, the type of their influence on the sediment dynamics needs to be further investigated. Sediment input and erosion are assumed to have reached an equilibrium state. The stability of this equilibrium must be further investigated. If changes occur, the management strategies need to be adjusted to adapt the transport capacity of the river appropriately.

Statistically significant differences in some geomorphic units were found between wide and narrow subreaches. The outcomes of the high-resolution imagery survey are condensed into a conceptual model. Narrow reaches are understood as transport efficient without major deposition, forming cascades of steps and pools. Deposition takes place in wide reaches, forming bars and islands. The distribution of geomorphic units is more affected in wide reaches.

This study has demonstrated the usefulness of unmanned aerial survey techniques to investigate river morphodynamics. It is crucial to understand river morphodynamics for regime-based river management. Drones and digital photogrammetry could be confirmed as a suitable method for monitoring geomorphology and physical river habitat. It will be further adapted within the long-term monitoring of fluvial morphology and related processes in the Spöl River.

7 Acknowledgement

I thank my supervisors, Dr. Virginia Ruiz-Villanueva, Prof. Fritz Schlunegger and Prof. Markus Stoffel for giving me the opportunity to expand on my knowledge in the field of river morphodynamics, river management and unmanned aerial surveys. A special thank goes to Dr. Virginia Ruiz-Villanueva for her investment and patience to help me through this thesis.

I am grateful to the Swiss academies of arts and science (ICAS), especially Thomas Scheurer, who enabled this project. A special thank goes to the Swiss National Park, especially Ruedi Haller, Samuel Wiesmann and Christian Rossi, for implementing the drone flights, providing me with information and valuable GIS datasets and for their readiness to help in any case. I thank the HYDRA Büro für Gewässerökologie Mürle und Ortlepp, especially Johannes Ortlepp, for the cooperation.

Furthermore, I acknowledge Dr. Marjorie Perroud (University of Geneva) and Gabriela Schär for their effort and assistance in the field. I thank Matthias Pfäffli for providing grain size data for comparison and Caro van Leeuwen for the improvement of the English text. I thank Dr. Romain Delunel for his help regarding struggles with ArcGIS and the Geographic Institut of the University of Bern, especially Prof. Dr. Margreth Keiler and Chantal Schmidt for providing us with technical equipment.

I am grateful to Sibylla Hardmeier and my husband, Philipp Schläfli, for enduring my moods and being on the spot with constructive words and optimism.

8 References

- Abbe, T. B., and Montgomery, D. R. (2003). Patterns and processes of wood debris accumulation in the Queets River Basin, Washington, *Geomorphology*, 51(1-3), 81–107, doi: 10.1016/S0169-555X(02)00326-4.
- Ackermann, G., Ortlepp, J., Pitsch, P., Rey, P., and Robin, K. (1996). Entleerung des Ausgleichsbecken Ova Spin 1995: Wie geht es der Pflanzen- und Tierwelt nach der Spülung. - *Cratschla*, 4 (2), 37-45.
- Adams, J. (1979). Gravelsize analysis from photographs. *Journal of the Hydraulics Division, American Society of Civil Engineers* 105: 1247-1285.
- agisoft.com (06.11.2017). Tutorial (Beginner level): Orthomosaic and DEM Generation with Agisoft PhotoScan Pro 1.3 (with Ground Control Points). Retrieved from <http://www.agisoft.com/support/tutorials/beginner-level/>
- Andrews, E. D., and Pizzi, L. A. (2000). Origin of the Colorado River experimental flood in Grand Canyon. *Hydrological Sciences* 45, 607–627.
- Bangen, S. G., Wheaton, J. M., Bouwes, N., Bouwes, B., and Jordan, C. (2014). A methodological intercomparison of topographic survey techniques for characterizing wadeable streams and rivers. *Geomorphology*, 206, 343–361. doi: 10.1016/j.geomorph.2013.10.010
- Bangen, S. G., Kramer, N., Wheaton, J.M., and Bouwes N. (2017). The GUTs of the Geomorphic Unit Tool: What is under the hood. EP31D-1901. AGU. New Orleans, LA, 11-15 Dec. doi: 10.13140/RG.2.2.31118.66884
- Bezzola, G. R. (2013). *Flussbau, Vorlesungsmanuskript [Book]*. Zürich: Versuchsanstalt für Wasserbau, ETH Zürich, FS 2013.
- Borselli, L., Cassi, P., and Torri, D. (2008). Prolegomena to sediment and flow connectivity in the landscape: A GIS and field numerical assessment. *Catena*, 75(3), 268–277.
- Brasington, J., Rumsby, B. T., and Mcvey, R. A. (2000). Monitoring and Modelling Morphological Change in a Braided Gravel-Bed River Using High Resolution Gps-. *Earth Surface Processes and Landforms*, 25, 973–990.
- Bravard, J.P., and Petts, G.E. (1996). Human impacts on fluvial hydrosystems. In: Petts, G.E., Amoros, C. (Eds.), *Fluvial Hydrosystems*. Chapman and Hall, London, 242–262.
- Brierley, G. J., and Fryirs, K. A. (2005). *Geomorphic Analysis of River Systems*. doi: 10.1029/2003WR002583.Bertoldi
- Buffington, J. M., and Montgomery, D. R. (2005). Geomorphic Classification of Rivers and Streams. In *Treatise on Geomorphology*, 9, 171–204. doi: 10.1002/0470868333.ch7
- Buffington, J. M. (2012). Changes in channel morphology over human time scales. In: Church, M., Biron, P.M., Roy, A.G. (Eds.), *Gravel-bed Rivers: Processes, Tools, Environments*. Wiley, Chichester, UK, 435–463.
- Cantonal Police Force Graubünden (04.11.2016). *Zernez: Bauschadstoffe im Spöl - Anzeige eingereicht*. Retrieved from <https://www.gr.ch/DE/institutionen/verwaltung/djsg/kapo/aktuelles/medien/2016/Seiten/201611042.aspx>

References

- Cavalli, M., Trevisani, S., Comiti, F., and Marchi, L. (2013). Geomorphometric assessment of spatial sediment connectivity in small Alpine catchments. *Geomorphology*, 188, 31–41. doi: 10.1016/j.geomorph.2012.05.007
- Cavalli, M., Crema, S., and Marchi, L. (2014). Guidelines on the Sediment Connectivity ArcGis Toolbox and stand-alone application, (June 2015), 32. doi: 10.13140/RG.2.1.3243.5361
- Church, M.A., McLean, D.G., and Wolcott, J.F. (1987). River bed gravels: sampling and analysis. In: Thorne, C.R., Bathurst, J.C., Hey, R.D., eds., *Sediment Transport in Gravel Bed Rivers*, New York: John Wiley and Sons, 43-79.
- Comiti, F. (2012). How natural are Alpine mountain rivers? Evidence from the Italian Alps. *Earth Surf. Process. Landf.* 37, 693–707.
- Crema, S., Schenato, L., Goldin, B., Marchi, L., and Cavalli, M. (2015). Toward the development of a stand-alone application for the assessment of sediment connectivity. *Rendiconti Online Societa Geologica Italiana*, 34, 58–61. doi: 10.33.01/ROL.2015.37
- Demarchi, L., Bizzi, S., and Piégay, H. (2016). Hierarchical object-based mapping of riverscape units and in-stream mesohabitats using lidar and VHR imagery. *Remote Sensing*, 8(2). doi: 10.3390/rs8020097
- Eberstaller, J., Frangez, C., and DiTullio, F. (2014). *Fischökologisches Monitoring Alpenrhein 2013*. Herausgeber: Internationale Regierungskommission Alpenrhein (IRKA).
- Eltner, A., Mulsow, C., Maas, H. G. (2013). Quantitative measurement of soil erosion from TLS and UAV data. In: *International Archives of the Photogrammetry, Remote Sensing and Spatial Information Sciences*, Volume XL-1/W2, UAV-g2013, Rostock, Germany, 4–6.
- Fehr, R. (1987). Einfache Bestimmung der Korngrößenverteilung von Geschiebematerial mit Hilfe der Linienzahlanalyse [Journal]. *Schweizer Ingenieur und Architekt, Abwassertechnik. Wasserbau. - Zürich*: [s.n.], 38/87, 1104-1109.
- Fonstad, M. A., Dietrich, J. T., Courville, B. C., Jensen, J. L. and Carbonneau, P. E. (2013). Topographic structure from motion: a new development in photogrammetric measurement. *Earth Surf. Process. Landforms*, 38, 421–430.
- Graf, W. L. (2006). Downstream hydrologic and geomorphic effects of large dams on American rivers. *Geomorphology* 79, 336–360.
- Groffman, P. M., Baron, J. S., Blett, T., Gold, A. J., Goodman, I., Gunderson, L. H., Levinson, B. M., Palmer, M. A., Paerl, H. W., Peterson, G. D., Poff, N. Le Roy, Rejeski, D. W., Reynolds, J. F., Turner, M. G., Weathers, K. C., and Wiens, J. (2006). Ecological thresholds: the key to successful environmental management or an important concept with no practical application? *Ecosystems* 9, 1–13.
- Grove, H. (1999). The importance of physical habitat assessment for evaluating river health. *Freshwater Biology*.
- Gurnell, A. M., Bussettini, M., Camenen, B., Tánago, M. G. Del, Grabowski, R. C., Hendriks, D., Henshaw, A., Latapie, A., Rinaldi, M., and Surian, N. (2014). A hierarchical multi-scale framework and indicators of hydromorphological processes and forms, (July 2015), 1–109. doi: D1.1

- Hajdukiewicz, H., Wyzga, B., Mikus, P., Zawiejska, J., and Radecki-Pawlik, A. (2016). Impact of a large flood on mountain river habitats, channel morphology, and valley infrastructure. *Geomorphology*, 272, 55–67. <https://doi.org/10.1016/j.geomorph.2015.09.003>
- Harper, D., Smith, C., Barham, P., and Howell, R. (1995). The ecological basis for the management of the natural river environment. *The Ecological Basis for River Management*. (Eds D.M. Harper, and A.J.D. Ferguson), 219-238. Wiley, Chichester.
- Hervouet, A., Dunford, R., Piegay, H., Belletti, B., Tremelo, M. L. (2011). Analysis of post-flood recruitment patterns in braided-channel rivers at multiple scales based on an image series collected by unmanned aerial vehicles, ultra-light aerial vehicles, and satellites. *GISci Remote Sens* 2011, 48, 50–73. doi: 10.2747/1548-1603.48.1.50.
- Hollander, M., and Wolfe D. A. (1999). *Nonparametric Statistical Methods*. Hoboken, NJ: John Wiley & Sons, Inc.
- Ibbeken, H., and Schleyer, R. (1986). Photo-sieving: a method for grain-size analysis of coarse-grained, unconsolidated bedding surfaces. *Earth Surfaces Processes and Landforms* 11, 59-77.
- Jochner, M., Turowski, J. M., Badoux, A., Stoffel, M., and Rickli, C. (2015). The role of log jams and exceptional flood events in mobilizing coarse particulate organic matter in a steep headwater stream. *Earth Surface Dynamics*, 3(3), 311–320. doi: 10.5194/esurf-3-311-2015
- Jowett, I.G. (1997). Instream flow methods: a comparison of approaches. *Regulated Rivers: Research and Management*, 13, 115-127.
- Keller, E. A., MacDonald, A., Tally, T., and Merritt, N. J. (1995). Effects of large organic debris on channel morphology and sediment storage in selected tributaries of Redwood Creek. U.S. Geological Survey Professional Paper 1454-P, Menlo Park, California.
- Kellerhals, R., and Bray, D.I. (1971). Sampling procedures for coarse fluvial sediments. *Journal of Hydraulics Division of the American Society of Civil Engineers* 97, 1165-1179.
- Kendall, M.G. (1970). *Rank Correlation Methods*. Griffin.
- Klein, R.D. (1987). Stream channel adjustments following logging road removal in Redwood National Park, MS Thesis, Humboldt State University, Arcata, California.
- Kondolf, G. M., Lisle, T. E., and Wolman, G. M. (2005). *Bed Sediment Measurement. Tools in Fluvial Geomorphology*. doi: 10.1002/0470868333.ch13
- Kramer, N., Bangen, S. G., Wheaton, J. M., Bouwes, N., Wall, E., Saunders, C., and Bennett S. (2017). Geomorphic Unit Tool (GUT): Applications in Fluvial Mapping. EP11A-1546. AGU. New Orleans, LA, 11-15 Dec. doi: 10.13140/RG.2.2.30142.18241
- Kruskal, W., and Wallis, W. (1952). Use of Ranks in One-Criterion Variance Analysis. *Journal of the American Statistical Association*, 47(260), 583-621. doi: 10.2307/2280779

References

- Ky.gov (28.02.2018). Pebble Count Analyzer.xlsx. Retrieved from <http://water.ky.gov/permitting/Lists/Individual%20Permit%20Documents/AllItems.aspx>
- Mannes, S., Robinson, C. T., Uehlinger, U., Scheurer, T., Ortlepp, J., Mürle, U., and Molinari, P. (2008). Ecological effects of a long-term flood program in a flow-regulated river, 2(2014), 1–12.
- McKean, J., and Isaak, D. (2009). Improving stream studies with a small-footprint green LiDAR. *Eos, Transactions, American Geophysical Union* 90, 341–342.
- Messenzehl, K., Hoffmann, T., and Dikau, R. (2014). Sediment connectivity in the high-alpine valley of Val Mueschauns, Swiss National Park - linking geomorphic field mapping with geomorphometric modelling. *Geomorphology*, 221, 215–229. doi: 10.1016/j.geomorph.2014.05.033
- MeteoSwiss (2018). Homepage of the Federal Office of Meteorology and Climatology MeteoSwiss. Available: <http://www.meteoschweiz.admin.ch/web/en.html> (26 April 2018).
- Mikuś, P., Wyzga, B., Kaczka, R.J., Walusiak, E., and Zawiejska, J. (2013). Islands in a European mountain river: linkages with large wood deposition, flood flow and plant diversity. *Geomorphology* 202, 115–127.
- Milhous, R. T. (1998). Modelling of instream flow needs: The link between sediment and aquatic habitat. *Regulated Rivers: Research and Management* 14, 79–94.
- Montgomery, D. R., and Buffington, J. M. (1997). Channel-reach morphology in mountain drainage basins. *Geological Society of America Bulletin* 109, 596–611.
- Mürle, U. (2000). Morphologie und Habitatstruktur in der Ausleitungsstrecke einer alpinen Stauhaltung (Spöl , Schweizerischer Nationalpark , Engadin), (April).
- Mürle, U., Ortlepp, J., and Zahner, M. (2003). Effects of experimental flooding on riverine morphology, structure and riparian vegetation: The River Spöl, Swiss National Park. *Aquatic Sciences*, 65(3), 191–198. doi: 10.1007/s00027-003-0665-6
- Nilsson, C., Reidy, C. A., Dynesius, M., and Revenga, C. (2005). Fragmentation and flow regulation of the world's large river systems. *Science* 308, 405–408.
- Ortlepp, J. and Mürle, U. (2003). Effects of experimental flooding on brown trout (*Salmo trutta fario* L.) *Aquat. Sci.* 65(3), 232–238.
- Parkforschung (01.04.2017). Long-term monitoring of fluvial morphology and related processes in the Spöl river (Swiss National Park) - Project Number: CH-6000. http://4dweb.proclim.ch/4dcgi/parkforschung/de/Detail_Project?ch-6000
- Petts, G. E. (1996). Water allocation to protect river ecosystems. *Regulated Rivers: Research and Management* 12, 353–365.
- Pfäffli, M. (2013). Sediment Dynamics Modelling in the River Spöl in the Swiss National Park.
- Puigdefabregas, J., Sole, A., Gutierrez, L., Del Barrio, G., and Boer, M. (1999). Scales and processes of water and sediment redistribution in drylands: results from the Rambla Honda field site in Southeast Spain. *Earth-Science Reviews* 48 (1–2), 39–70.

- Rey, P., and Hesselschwerdt, J. (2016). Monitoring Alpenrhein - Basismonitoring Ökologie 2015. Herausgeber: Internationale Regierungskommission Alpenrhein (IRKA).
- Rey, P. and Hesselschwerdt, J. (2017). Habitatflächen am Alpenrhein: Methodenvorschlag zur Erfassung, Quantifizierung und Bewertung von Flussraumstrukturen anhand von Luftbildern.
- Rice, S., and Church, M. (1998). Grain size along two gravel-bed rivers: statistical variation, spatial pattern and sedimentary links. *Earth Surface Processes and Landforms* 23, 345-363.
- Robinson, C. T., and Uehlinger, U. (2006). Experimental Floods Cause Ecosystem Regime Shift, 00(2), 511–526.
- Ruiz-Villanueva, V., Piégay, H., Gurnell, A. A., Marston, R. A., and Stoffel, M. (2016). Recent advances quantifying the large wood dynamics in river basins: New methods and remaining challenges. *Reviews of Geophysics*, 54(3), 611–652. doi: 10.1002/2015RG000514
- Scheffer, M., Carpenter, S., Foley, J. A., Folke, C., and Walker, B. (2001). Catastrophic shifts in ecosystems. *Nature* 413, 591–596.
- Scheurer, T., and Molinari, P. (2003). Experimental floods in the River Spoel, Swiss National Park: Framework, objectives and design. *Aquatic Sciences*, 65(3), 183–190. doi: 10.1007/s00027-003-0667-4
- Schmidt, J. C., Parnell, R. A., Grams, P. E., Hazel, J. E., Kaplinski, M. A., Stevens, L. E., and Hoffnagle, T. L. (2001). The 1996 controlled flood in the Grand Canyon: flow, sediment transport and geomorphic change. *Ecological Applications* 11: 657–671.
- Schweizerischer Bund für Naturschutz (HRSG.) (1947). Nationalpark oder internationales Spölkraftwerk - Stimmen zur Erhaltung des Schweizerischen Nationalparks im Unterengadin. - Schweizerische Naturschutzbücherei.
- Snavely, N., Seitz, S. M., and Szeliski, R. (2006). PhotoTourism: Exploring Photo Collections in 3D. *SIGGRAPH Conference Proceedings*, 835-846. doi: 10.1145/1141911.1141964
- Snavely, N., Garg, R., Seitz, S. M., and Szeliski, R. (2008). Finding paths through the world's photos. *ACM Transactions on Graphics*, 27(3), 1. doi: 10.1145/1360612.1360614
- Snavely, N. (2008). Scene Reconstruction and Visualization from Internet Photo Collections. Doctoral thesis, University of Washington.
- Standeskanzlei Graubünden (22.12.2016). Bauschadstoffe im oberen Spöl. Retrieved from <https://www.gr.ch/DE/Medien/Mitteilungen/MMStaka/2016/Seiten/2016122203.aspx>
- Stanford, J. A., Ward, J. V., Liss, W. J., Frissell, C. A., Williams, R. N., Lichatowich, J. A., and Coutant, C. C. (1996). A general protocol for restoration of regulated rivers. *Regulated Rivers: Research and Management* 12: 391–413.
- Surian, N., Barban, M., Ziliani, L., Monegato, G., Bertoldi, W., and Comiti, F. (2015). Vegetation turnover in a braided river: frequency and effectiveness of floods of different magnitude. *Earth Surf. Process. Landf.* 40, 542–558.

References

- Swiss National Park (15.03.2018). Bauschadstoffe im oberen Spöl - mögliche Sanierungsmassnahmen in Abklärung. Retrieved from <http://www.national-park.ch/de/about/mediencorner/medienmitteilungen/medienmitteilungen-2017/bauschatstoffe-im-oberen-spoel-moegliche-sanierungsmassnahmen-in-abklaerung/>
- Tarboton, D.G. (2012). TauDEM 5.0. Terrain analysis using digital elevation models, (Available: <http://www.engineering.usu.edu/dtarb/taudem> (19 June 2013)).
- Thiel, M., Heckmann, T., Haas, F., and Becht, M. (2011). Quantification of coarse sediment connectivity in alpine geosystems. *Geophysical Research Abstracts* 13 (EGU2011-10449).
- Trevisani, S., and Cavalli, M. (2016). Topography-based flow-directional roughness: potential and challenges. *Earth Surface Dynamics*, 343–358. doi: 10.5194/esurf-4-343-2016
- Uehlinger, U., Kawecka, B., and Robinson, C. T. (2003). Effects of experimental floods on periphyton and stream metabolism below a high dam in the Swiss Alps (River Spoel). *Aquatic Sciences*, 65(3), 199–209. doi: 10.1007/s00027-003-0664-7
- Vinson, M. R. (2001). Long-term dynamics of an invertebrate assemblage downstream of a large dam. *Ecological Applications* 11, 711–730.
- Wallace, J. B. (1990). Recovery of lotic macroinvertebrate communities from disturbance. *Environmental Management* 14, 605–620.
- Ward, J. V., and Stanford, J. A. (1979). *The ecology of regulated streams*. Plenum Press, New York, New York, USA.
- Wheaton, J. M., Fryirs, K. A., Brierley, G. J., Bangen, S. G., Bouwes, N., and O'Brien, G. (2015). Geomorphic mapping and taxonomy of fluvial landforms. *Geomorphology*, 248(November), 273–295. doi: 10.1016/j.geomorph.2015.07.010
- Wichmann, V., Heckmann, T., Haas, F., and Becht, M. (2009). A new modelling approach to delineate the spatial extent of alpine sediment cascades. *Geomorphology* 111, 70–78.
- Wissenschaftliche Nationalparkkommission (WNPK) (HRSG.) (1991). *Wissenschaftliche Begleitung Spülung Grundablass Livigno-Stausee vom 7. Juni 1990. - Arbeitsberichte zur Nationalparkforschung*, 1-5, 319-342
- Wohl, E. (2006). Human impacts to mountain streams. *Geomorphology* 79, 217–248.
- Wohl, E., Cenderelli, D. A., Dwire, K. A., Ryan-Burkett, S. E., Young, M. K., and Fausch, K. D. (2010). Large in-stream wood studies: A call for common metrics. *Earth Surface Processes and Landforms*, 35(5), 618–625. doi: 10.1002/esp.1966
- Wohl, E., and Scott, D. N. (2016). Wood and sediment storage and dynamics in river corridors. *Earth Surface Processes and Landforms*. doi: 10.1002/esp.3909
- Woodget, A. S., Austrums, R., Maddock, I. P., and Habit, E. (2017). Drones and digital photogrammetry: from classifications to continuums for monitoring river habitat and hydromorphology. *Wiley Interdisciplinary Reviews: Water*, 4(4), e1222. doi: 10.1002/wat2.1222
- World Commission on Dams (2000). *Dams and development: a new framework for decision-making*. Earthscan Publications, London, UK.

- Wyzga, B., Mikus, P., Zawiejska, J., Ruiz-Villanueva, V., Kaczka, R. J., and Czech, W. (2015). Log transport and deposition in incised, channelized, and multithread reaches of a wide mountain river: Tracking experiment during a 20-year flood. *Geomorphology*, 279, 98–111. doi: 10.1016/j.geomorph.2016.09.019

9 Appendix



Figure 38: Hydrograph of Station “Punt dal Gall” from 19. – 20.06.2009. The time span of the shot of the orthomosaic 2009 is highlighted. (Pfäffli, 2003)

9.1 Digital Appendix

An extended appendix is provided on the enclosed data medium:

Table 8: Overview of the digital appendix

Folder	Documents	Contents
1_FieldMeasurements	Field_protocols.docx	Compilation of the used protocols for field-work
	fielddata.lpk	GIS data of field measurements
	fielddata_20170907_complete.xlsx	Compilation of GPS and field measurements
2_HistoricalAnalysis	Orthomosaics	folder with orthomosaics from 1946, 1988, 2000, 2009, 2010 and 2013, including back-ground information
	historical_analysis.lpk	shapefiles with the mapped geomorphic units (points and polygons) for each orthomosaic, respectively
	SR_analysis.xlsx	Compilation of the remotely mapped units
	SR_analysis_trib.xlsx	Geomorphic units up- and downstream the tributaries Acqua and Foeglia
	SR_analysis_widthvalleyfan.xlsx	Valley width and fan width
3_SedimentConnectivity	Connectivity.rar	Inputs and Results of the SedIn Connect tool
	SedInConnectivity.xlsx	protocol to the Connectivity analysis with the SedIn Connect tool
4_GrainSizeAnalysis	GSDplots	folder with matlab plots of the grain size distribution samples from Pfäffli (2003) and this study

	fielddata_grainsize.xlsx	Compilation of the GSD results from ImageJ and data from Pfäffli (2003)
	ImageJ_Tutorial.docx	Step by step guide for grain size analysis with ImageJ
	Pebble Count Analyzer.xlsx	Calculator for GSD, provided by Ky.gov (28.02.2018)
5_AerialSurvey	Flightplans	folder with the AscTec Navigator flight plans and background information to the flights
	Photogrammetry	folder with the Agisoft processing report and a process documentation
	spoel2017_DSM	Photogrammetry output DSM
	spoel2017_ortho	Photogrammetry output orthomosaic
6_Other	Information_brochure_SNP.pdf	Information brochure of the Swiss National Park

9.2 List of Figures

Figure 1: Overview of the study site (red rectangle) and surroundings (Scheurer and Molinari, 2003)	6
Figure 2: Longitudinal profile of the upper Spöl River from Punt dal Gall to Ova Spin	6
Figure 3: Geological map of the study area (swisstopo). The black rectangle highlights the outlets of Acqua and Foeglia (in flow direction) into the studied river reach	7
Figure 4: Corine Landuse Cover map for the catchment of the Spöl River on swiss ground, a black line contours the reach from the dam Punt dal Gall to the reservoir lake Ova Spin	8
Figure 5: Impressions of the Spöl River, a-b) pool-riffle and steps, c-d) fans, e-f) canyons	8
Figure 6: Flow regime of the Spöl River before dam construction (1961 and 1962), after dam construction (1999) and during the flood program (2000-2006). The flow in 1999 represents the residual flow maintained below the dam with all excess water diverted downstream for power production (Mannes et al., 2008)	9
Figure 7: General flow chart with the applied approach	10
Figure 8: Classification framework	12
Figure 9: Example of the mapped units in the Spöl River (without ICF)	12
Figure 10: Field measurements for validating the remotely mapped units (a) boulder dimensions and wood jam, b) pool depth, c) wood log, d) subreach boundary	14
Figure 11: Upslope and downslope components of the IC (Cavalli et al., 2014)	16
Figure 12: Example of a GSD picture with the overlying grid in ImageJ	18
Figure 13: Flight plan in AscTec Navigator	20

Figure 14: Fieldwork with the drone: a)-b) AscTec Falcon 8 octocopter, c) starting the drone by hand, d) remote control of the previously planned flight, e)-f) GCP installation and measuring	21
Figure 15: Post-processing of the aerial imagery in Agisoft Photoscan	22
Figure 16: Area of the water channel, sediment bars and fans over time. The blue bars show the annual maximum discharge.	23
Figure 17: Relative proportions of the units forming the TAC in the considered years	24
Figure 18: Development of a fan (indicated with a red arrow) from 1946 to 2017. The fan propagates into the active channel until the flood program gets started in 2000. From then the fan area slightly decreases, but the vegetated parts (red circle) remain vegetated. The blue arrow indicates flow direction.	25
Figure 19: Relative proportions of the subunits forming the water channel (upper left), the sediment bars (upper right) and the vegetated areas (lower left). Classification code for Water channel units: uncW = unclassified water surface, Wf = Waterfall, StW = Standing Water, Ru = Run, P = Pool, Ri = Riffle; Classification code for Sediment bars: pb = point bar, mcb = mid-channel bar, lb = lateral bar; Classification code for Vegetated area: DVI = Densely-Vegetated units of Islands, RDV = Riparian Densely-Vegetated units, SVI = Sparsely-Vegetated units of Islands, RSV = Riparian Sparsely-Vegetated units	26
Figure 20: Channel width along the studied reach from 1946 to 2017. Results of the Kruskal-Wallis test for the significance of differences in the width between time sequential pair of years are also indicated. p values < 0.05 are indicated in bold.	27
Figure 21: Comparison of width measurements in the field with remote width measurements on the orthomosaics in ArcGIS. The linear regression equation, as well as the coefficient of determination R^2 , are indicated. The p-value of the Spearman test indicates the significance of the correlation between field and remote measurements. p values < 0.05 are indicated in bold.	27
Figure 22: Classified map of the index of connectivity for the upper Spöl River with fans as sediment source areas. Left: Spöl River as a target. Right: including channels of the most important tributaries as a target, namely Acqua and Foeglia (in flow direction).	28
Figure 23: Overview of the GSD samples along the river reach. The points describe the characteristic grain diameter d_m and d_{90} of the samples from this study as well as the results from Pfäffli (2013). The dashed line illustrates the mean values from samples laying close together. Fans and tributaries are indicated with orange and blue bars, respectively. The main tributaries Acqua and Foeglia river are indicated as well.	29
Figure 24: Grain diameter d_m and d_{90} of the samples from 2013 (Pfäffli, 2013) and this study (2017). Results of the Mann-Whitney test indicate the significance of differences between the data sets. p values < 0.05 are indicated in bold.	29
Figure 25: Section of the orthomosaic and DSM generated using the drone Structure-from-Motion approach (SfM)	31

Figure 26: GCP location and error estimates from the Agisoft Processing Report (see Appendix)	32
Figure 27: Orthomosaic section (left) and drone image (right) at GCP p48 (marked with a red circle)	32
Figure 28: Geomorphic map of the upper Spöl River	33
Figure 29: Overview of the heterogeneous spatial distribution of some selected geomorphic units along the studied reach of the upper Spöl River	34
Figure 30: Subdivision of the studied reach into subreaches according to the channel width. Subreaches with a mean channel width > total mean channel width are classified as “wide” (grey background), the others are classified as “narrow”. Mean channel width is indicated with a black horizontal line.	34
Figure 31: Subdivision of the studied reach into subreaches according to the channel slope. Subreaches with a mean channel slope > total mean channel slope are classified as “steep” (grey background), the others are classified as “shallow”. Mean channel slope is indicated with a black horizontal line. A red vertical line marks the splitting of the studied reach at the outlet of the Acqua river into upstream Acqua and downstream Acqua.	35
Figure 32: Range and mean values of mapped units along the Spöl River for wide and narrow subreaches. Subreaches with a mean channel width > total mean channel width are categorized as wide and otherwise as narrow (Figure 30). Statistical significance can be found in Table 6.	37
Figure 33: Range and mean values of mapped units along the Spöl River for steep and shallow subreaches. Subreaches with a mean channel slope > total mean channel slope are categorized as steep and otherwise as shallow (Figure 31). Statistical significance can be found in Table 6.	38
Figure 34: Range and mean values of mapped units along the Spöl River up- and downstream the outlet of the Acqua river, here referred to as “upstream” and “downstream”, respectively. Statistical significance can be found in Table 6.	39
Figure 35: Comparison of particular mapped units. p-values < 0.05 are indicated in bold.	40
Figure 36: Conceptual model of the upper Spöl River showing the characteristics of wide and narrow subreaches	50
Figure 37: Concept of habitat as the natural link between the physical environment and its inhabitants (Harper et al., 1995)	52
Figure 38: Hydrograph of Station “Punt dal Gall” from 19. – 20.06.2009. The time span of the shot of the orthomosaic 2009 is highlighted. (Pfäffli, 2003)	62

9.3 List of Tables

Table 1: river parameters	6
Table 2: Overview of the analysed orthomosaics with project parameters	11
Table 3: Classification scheme, adapted from Demarchi et al. (2016)	13
Table 4: Subreach description	15

Appendix

Table 5: Survey data from the Agisoft Processing Report (see Appendix)	30
Table 6: Results of the Kruskal-Wallis Test indicating the statistical significance of the difference of particular mapped units between the subreach type pairs (wide-narrow, steep-shallow, up- and downstream Acqua). p-values < 0.05 are highlighted in bold.	36
Table 7: Range and mean values of the confinement index for wide and narrow subreaches and the entire studies reach	36
Table 8: Overview of the digital appendix	62

Declaration of consent

on the basis of Article 28 para. 2 of the RSL05 phil.-nat.

Name/First Name: Schläfli Salome

Matriculation Number: 11-802-246

Study program: Earth Sciences

Bachelor ☐

Master ☒

Dissertation ☐

Title of the thesis: Regulated flows influence on river morphodynamics: The Spöl River
(Swiss National Park)

Supervisor: Prof. Fritz Schlunegger
Prof. Markus Stoffel
Dr. Virginia Ruiz-Villanueva

I declare herewith that this thesis is my own work and that I have not used any sources other than those stated. I have indicated the adoption of quotations as well as thoughts taken from other authors as such in the thesis. I am aware that the Senate pursuant to Article 36 para. 1 lit. r of the University Act of 5 September, 1996 is authorised to revoke the title awarded on the basis of this thesis. I allow herewith inspection in this thesis.

Zofingen, 20.08.2018

Place/Date

Signature

